Meteoric ^{10}Be as a tracer of subglacial processes and interglacial surface exposure in Greenland

Joseph A. Graly[1], Lee B. Corbett[2], Paul R. Bierman[2], Andrea Lini[2], Thomas A. Neumann[3]

1: Indiana University Purdue University Indianapolis, Dept. of Earth Sciences, Indianapolis, IN, USA

2: University of Vermont, Dept. of Geology, Burlington, VT, USA

3: NASA Goddard Space Flight Center, Greenbelt, MD, USA

Keywords: Quaternary; Interglacials; Glaciation; Glaciology; Greenland; Cosmogenic isotopes; Stable isotopes.

Abstract: In order to test whether sediment emerging from presently glaciated areas of Greenland was exposed near or at Earth's surface during previous interglacial periods, we measured the rare isotope ^{10}Be contained in grain coatings of sediment collected at five ice marginal sites. Such grain coatings contain meteoric ^{10}Be ($^{10}Be_{met}$), which forms in the atmosphere and is deposited onto Earth's surface. Samples include sediment entrained in ice, glaciofluvial sediment collected at the ice margin, and subglacial sediment extracted during hot water drilling in the ablation zone. Due to burial by ice, contemporary subglacial sediment could only have acquired substantial $^{10}Be_{met}$ concentrations during periods in the past when the Greenland Ice Sheet was less extensive than present.

The highest measured $^{10}Be_{met}$ concentrations are comparable to those found in well-developed, long-exposed soils, suggesting subglacial preservation and glacial transport of sediment exposed during preglacial or interglacial periods. Ice-bound sediment has significantly higher $^{10}Be_{met}$ concentrations than glaciofluvial sediment, suggesting that

This is the author's manuscript of the article published in final edited form as:
Graly, J. A., Corbett, L. B., Bierman, P. R., Lini, A., & Neumann, T. A. (2018). Meteoric 10Be as a tracer of subglacial processes and interglacial surface exposure in Greenland. Quaternary Science Reviews, 191, 118–131. https://doi.org/10.1016/j.quascirev.2018.05.009

glaciofluvial processes are sufficiently erosive to remove tracers of previous interglacial exposures. Northern Greenland sites where ice and sediment are supplied from the ice sheet's central main dome have significantly higher $^{10}Be_{met}$ concentrations than sites in southern Greenland, indicating greater preglacial or interglacial landscape preservation in central Greenland than in the south. Because southern Greenland has more frequent and spatially extensive periods of glacial retreat but nevertheless has less evidence of past subaerial exposure, we suggest that $^{10}Be_{met}$ measurements in glacial sediment are primarily controlled by erosional efficiency rather than interglacial exposure length.

Introduction

For ice sheets, such as the Greenland Ice Sheet, the links between climate forcings, ice sheet response, and resultant sediment fluxes has generally not been well resolved (Bierman et al., 2016). Past interglacial periods, such as the mid-Holocene and marine isotope stage (MIS) 5e, had reduced global ice volumes compared to present (Lisiecki and Raymo, 2005), but it remains uncertain how much of the ice volume change came from changes to the Greenland Ice Sheet (e.g. Stone et al., 2013). The sediment flux from erosion under glaciers and ice sheets is highly variable, with some regions experiencing considerable erosion (Hallet et al., 1996) and others experiencing very little (Bierman et al., 1999). Over the Quaternary period, substantial volumes of sediment have fluxed from the Greenland Ice Sheet to the oceans and shelf, although the total volume and chronology is not well constrained (Laine, 1980; Molnar, 2004). Modeling efforts can produce variable results depending on the assumed climate forcings (Goelzer et al., 2013) and have only

limited constraint from the offshore sediment record (Dowdeswell et al., 2014). New approaches for assessing past changes in ice sheet extent in and erosive response are needed.

Here, we seek to add new constraints on the past exposure history and erosive behavior of the Greenland Ice Sheet by measuring isotopic and geochemical tracers of previous surface exposure. Our study is based on the premise that analyses of previously exposed sediment at the present-day glacial margin can identify up-glacier regions where the ice sheet was previously absent and subsequent erosion was insufficient to fully remove such tracers from the landscape and thus from the ice sheet's sediment load. Meteoric ^{10}Be ($^{10}Be_{met}$) is the primary tracer we employ; it is a long-lived cosmogenic isotope that is easily incorporated into the grain coatings of sediment and accumulates during periods of surface exposure (Graly et al., 2010; Pavich et al., 1984). We also report organic carbon and total nitrogen measurements as indicators of soil formation and thus surface exposure (Barjes, 1996). We measured the stable isotope composition of water in the ice surrounding some of our samples in order to infer sediment entrainment mechanisms and therefore erosional processes (Sugden et al., 1987).

Background

Glacial-Interglacial History

The Greenland Ice Sheet is assumed to have responded to the same climate forcings that cause global glacial-interglacial cycles (Huybrechts, 2002), but the differences between Greenland's response and global average response are not known (Schaefer et al., 2016). According to the marine benthic stable isotope record, global ice volume was less than the mid-Holocene level for only ~40,000 of the past 2.1 million years (Bintanja and

van de Wal, 2008). This brevity of past interglacial global ice volume lows is independently confirmed by a variety of paleoclimatic indicators, such as speleothems, pelagic dust flux, and coastal highstand features (e.g. Grant et al., 2014; Rohling et al., 2017). In some cases, these records suggest even briefer interglacial highstands than the marine benthic stable isotope record implies (Rohling et al., 2010). This corresponds with a comparable lack of evidence of extended surface exposure after ~1.8 Ma in East Greenland's offshore record (Bierman et al., 2016). However, other evidence suggests the Greenland Ice Sheet may have been more responsive to climatic optima than the global records suggest. Measurement of ^{10}Be and ^{26}Al in cores of the sub-ice rock below the GISP2 ice core are consistent with either numerous or extensive periods of interglacial exposure in central Greenland, beginning in the mid-Pleistocene (Schaefer et al., 2016). Organic carbon and meteoric ^{10}Be in the basal sediment of the GISP2 core suggest preservation of a well-developed preglacial or interglacial soil in central Greenland (Bierman et al., 2014). Mid to later Pleistocene climatic optima are suggested by the presence of boreal-forest remains in sub-ice sediment from southern Greenland (Willerslev et al., 2007).

Meteoric ^{10}Be systematics

High concentrations of $^{10}Be_{met}$ are generally found in the chemically weathered portions of well-developed soils. $^{10}Be_{met}$ forms in the atmosphere from the spallation of nitrogen and oxygen by cosmic rays and has production rates on the order of 10^6 atoms·cm^{-2}·a^{-1}; it differs in production location from *in situ* ^{10}Be, which forms from atomic spallation within mineral lattices and has depth integrated production rates at sea level on the order of 10^3 atoms·cm^{-2}·a^{-1} (Lal and Peters, 1967). Once formed, $^{10}Be_{met}$ sorbs to aerosol

particles and is transported by atmospheric circulation, eventually coming to Earth through wet or dry deposition (Graly et al., 2011; Heikkilä et al., 2008). In general, $^{10}Be_{met}$ strongly adsorbs to sediment (You et al., 1989) and accumulates within the soil column (Pavich et al., 1984). However, Be is mobile, moving between adsorbed, clay, oxide, or oxyhydroxide phases with evolving soil chemistry (Bacon et al., 2012; Barg et al., 1997), typically following clay illuviation to accumulate in greatest concentrations within the B-horizon at depths < 2-3 m (Graly et al., 2010). In deep continental regolith, appreciable concentrations of meteoric ^{10}Be are found to depths of 10-20 m (Brown et al., 1988).

If similar deeply weathered regolith formed in preglacial Greenland, any regolith remaining after glaciation likely contains at least some $^{10}Be_{met}$. In contrast, the duration of brief interglacial periods (<10 ka) is insufficient for substantial clay illuviation or transport of $^{10}Be_{met}$ beyond the top meter of the soil profile (Harden et al., 2002; Pavich and Vidic, 1993). Though the systematics of $^{10}Be_{met}$ in soils have been mostly studied in the mid-latitudes, $^{10}Be_{met}$ data from high latitudes also show long-term transport of the isotope to depth (Ebert et al., 2012). High latitude flux of $^{10}Be_{met}$ to marine sediment has been measured in glaciomarine settings near Greenland and Antarctica, though its relationship to terrestrial soil concentrations is complicated by the scavenging of $^{10}Be_{met}$ from ocean water (Simon et al., 2016; Sjunneskog et al., 2007; Yokoyama et al., 2016).

Past studies have analyzed $^{10}Be_{met}$ concentrations in terms of a total soil inventory that uses the total abundance of the isotope within a soil column to assess surface ages and erosion rates (e.g. Pavich et al., 1986). The $^{10}Be_{met}$ inventory is related to soil exposure age via:

$$N = \frac{q}{\lambda}(1 - e^{-\lambda t}) \quad (1)$$

where N is the inventory measured in atoms·cm^{-2}, t is the exposure period in years, λ is the ^{10}Be disintegration constant of 5.0·10^{-7} yr^{-1} (Korschinek et al., 2010), and *q* is the average annual flux (atoms·cm^{-2}·a^{-1}) of ^{10}Be$_{met}$ atoms into the soil profile.

Holocene ^{10}Be$_{met}$ deposition rates in central Greenland are approximately 3.5·10^{5} atoms·cm^{-2}·a^{-1} based on measurements of ^{10}Be$_{met}$ in ice cores (Finkel and Nishiizumi, 1997). In eastern and southern Greenland, Holocene ^{10}Be$_{met}$ fluxes are up to 2 times larger, primarily due to higher mean annual precipitation (Sturevik-Storm et al., 2014). Eemian (MIS 5e) deposition rates were 30% higher; ~4.2·10^{5} atoms·cm^{-2}·a^{-1} is recorded in the NEEM core, in north-central Greenland (Sturevik-Storm et al., 2014). The Eemian ^{10}Be$_{met}$ data plot along the same accumulation-flux trend that is seen in the Holocene data, strongly suggesting that the increase in ^{10}Be$_{met}$ deposition is precipitation controlled. We do not know how closely the ^{10}Be$_{met}$ deposition rates of previous interglacial periods resembled mid-Holocene or Eemian fluxes.

Because ^{10}Be$_{met}$-bearing aerosols and dust are deposited on the ice sheet (Baumgartner et al., 1997), glacial ice is also a potential source of ^{10}Be$_{met}$ to the subglacial environment. In the ice sheet ablation zone, surface meltwater is routed to the bed and forms high discharge, erosive streams (Alley et al., 1997). Such streams are likely to erode and transport the subglacial sediment they encounter, and therefore are not likely to be a major source of ^{10}Be$_{met}$ to subglacial sediment. In regions where surface melt water does not readily reach the bed, basal melt is the only source of subglacial water. With geothermal heat fluxes implying basal melt rates of ~5 mm·a^{-1} (Greve, 2005), ice density of 0.9 g·cm^{-1}, and Pleistocene ^{10}Be$_{met}$ concentrations in ice of ~4·10^{4} atoms·g^{-1} (Finkel and Nishiizumi, 1997), the flux of ^{10}Be$_{met}$ from basal melt is approximately 1.8·10^{4} atoms·cm^{-2}·yr^{-1}. This

is more than an order of magnitude lower than the interglacial $^{10}Be_{met}$ flux from precipitation at the ice sheet surface documented in ice cores. Because surface $^{10}Be_{met}$ primarily runs off in erosive meltwater streams that would remove sediments that acquire the isotope and basal $^{10}Be_{met}$ is fluxed to the bed in minimal quantities, we conclude that $^{10}Be_{met}$ in sub-ice sediment will predominately accumulate during interglacial surface exposure or else be inherited from preglacial regolith (Figure 1).

Subglacial Processes

Soil, sediment, and rock at the ice sheet's bed may be transported by glaciofluvial subglacial streams, subglacial till shearing, or by sliding of basal ice that has entrained debris through refreezing processes (Alley et al., 1997). At the ice sheet margins, sediment carried by water and bound in ice are the major components of sediment flux (Knight, 1997; Knight et al., 2002). Subglacial fluvial processes have the greatest erosive power and have water and sediment residence times of hours to days (Alley et al., 1997; Chandler et al., 2013). Ice-bound sediment is transported by basal sliding, which is typically on the order of 10 $m \cdot a^{-1}$, but varies substantially both spatially and temporally, in that major outlet glaciers and large melting events induce substantial sliding accelerations (Joughin et al., 2008; Joughin et al., 2010). Residence times of sediment in basal ice layers are therefore on the order of 10^3 to 10^4 years when sediment is transported over distances on the scale of tens to hundreds of km. Sediment is incorporated into the basal ice layer through regelation (Hubbard and Sharp, 1993; Philip, 1980) or freeze-on (Alley et al., 1998), and can be released from the basal ice layer if the basal melt rate exceeds the rate of freeze-on. If the hydrologic and glaciological conditions allow for the transfer of sediment between

the basal ice layer and underlying till, the total sediment transport time from the point of origin to the margin may be longer than the transport time of basal ice.

The history and origin of the preglacial or interglacial soil material collected at the margin differ appreciably between ice-bound and glaciofluvial sediment samples. During regelation entrainment, ice-bound sediment is not completely homogenized by the entrainment mechanism, as the freezing front either advances or retreats through a static sediment profile based on thermal and glaciological factors (Rempel, 2008). This suggests that the ice-bound sediment samples may represent discrete natural sampling of the underlying sediment, and a $^{10}Be_{met}$ measurement could represent a preserved point in the soil column from a preglacial landscape. In contrast, glaciofluvial samples are likely to be integrated from a range of sediment depths and distances from the current ice margin (Walder and Fowler, 1994), and result in $^{10}Be_{met}$ concentrations that are spatially averaged over the catchment area of the subglacial stream. Sampling detrital material imparts only an imperfect knowledge of the transport and source histories; material we analyzed could have been sheared as till prior to regelation entrainment, or entrained for a time prior to basal melting and fluvial transport.

The process of regelation creates ice that is often enriched in heavy stable isotopes of oxygen and hydrogen compared with the water from which it is derived (Jouzel and Souchez, 1982). Past studies of marginal basal ice in western Greenland have primarily found isotopic patterns consistent with regelation entrainment in an open system, with loss of residual meltwater to the basal hydraulic system (Knight, 1989; Sugden et al., 1987). Due to the mass difference between heavy and light isotopes of O and H, the open system regelation enrichment effect is more strongly expressed by $\delta^{18}O$ than $\delta^{2}H$, resulting in

shallower two-isotope slopes than are found in meteoric water (Jouzel and Souchez, 1982). Experimental and theoretical findings predict that open-system regelation of Greenland Ice Sheet ice would produce a $\delta^2H/\delta^{18}O$ enrichment trend with a slope of approximately 5.5-6.0, depending on the initial isotopic composition of the ice (Iverson and Souchez, 1996; Lehmann and Siegenthaler, 1991). Based on the $\delta^2H/\delta^{18}O$ enrichment slope of 8 found in precipitation (Craig, 1961), deuterium excess is defined as $\delta^2H - 8 \cdot \delta^{18}O$. Excess values of 10 are considered typical of meteoric precipitation (Dansgaard, 1964); excess values found in regelation enriched ice are well-below meteoric values (Sugden et al., 1987).

Study Sites

Samples were collected from five study areas in coastal Greenland: Upernavik (72.6º N, 53.6º W), Illulisat (69.4º N, 50.3º W), Kangerlussuaq (67.1º N, 50.0º W), Tasiilaq (65.6º N, 38.5º W), and Narsarsuaq (61.2º N, 45.0º W) (Figure 2). Samples from Upernavik and Ilulissat were collected from flowlines that drain the main dome of the Greenland Ice Sheet to the west and originate near Summit. The Tasiilaq and Kangerlussuaq samples are from flowlines that drain the southern dome from the east and west sides respectively; Narsarsuaq is in the far south. All samples were collected from land-terminating ice. At sites that contain major marine-terminating outlet glaciers, such as Ilulissat and Tasiilaq, our samples were collected from smaller, land-terminating sites.

There is substantial variation in topographic character between the five sites. Both Upernavik and Narsarsauq are characterized by deep fjords dissecting relatively level uplands. At Upernavik, relief is on the order of 1000 m; at Narsarsuaq, relief is on the order of 1500 m. Ilulissat and Kangerlussuaq contrast with these sites; they are characterized by

210 a low relief (<500 m) landscape of glacially rounded hills. Tasiilaq is intermediate to the
211 other sites, both in relief and in dissection of the landscape.

212 The upland areas of the high-relief sites are generally consistent with minimal
213 glacial erosion. In the Upernavik area, the upland bedrock has a complex *in situ*
214 cosmogenic isotope exposure history, indicating subglacial erosion rates insufficient to
215 remove rock material at appreciable rates (Corbett et al., 2013). Low rates of subglacial
216 erosion are also suggested by the uplands' highly weathered rock surfaces, including
217 exfoliation sheets, tors, and weathering pits. Some of the highest elevation sites between
218 Kangerlussuaq and the coast also have 10^5 year *in situ* cosmogenic isotope histories, though
219 most of the landscape records only Holocene exposure due to efficient subglacial erosion
220 during the last glacial period (Rinterknecht et al., 2009; Roberts et al., 2009). Ilulissat lacks
221 substantial inheritance of *in situ* cosmogenic nuclides from prior periods of exposure, thus
222 indicating deep erosion during glaciation, even in upland areas (Corbett et al., 2011).
223 Though cosmogenic isotope measurements in the upland bedrock of Narsarsuaq suggest
224 only Holocene exposure, *in situ* ^{10}Be concentrations in fluvial sediment from non-glaciated
225 catchments draining upland areas found higher concentrations near Narsarsuaq than near
226 Tasiilaq or Kangerlussuaq (Nelson et al., 2014). The Narsarsuaq fluvial sediment sample
227 from the non-glacial stream with the highest *in situ* ^{10}Be concentration was included in this
228 study (GLX18).

229 Low-lying regions and fjords at all of the study sites appear to have simple
230 exposure histories that indicate rapid ice sheet retreat between 9 and 11 ka (Carlson et al.,
231 2014; Corbett et al., 2013; Kelley et al., 2013; Roberts et al., 2008), though early to middle
232 Holocene minor readvances are suggested at some sites (e.g. Carlson et al., 2014; Levy et

al., 2012; Young et al., 2013). Where the upland and lowland histories differ, it is likely that cold-based ice preserved the landscape on the highlands, while warm-based ice carved the fjords.

The sites also differ in distance from the ice sheet margin to the coast, both presently and in past interglacial periods. The Kangerlussuaq region is presently the furthest from the coast (~150 km), and most models show significant retreat in this sector of the Greenland Ice Sheet both during the mid-Holocene and the MIS 5e interglacial periods (Stone et al., 2013). The high relief sites (Upernavik and Narsarsuaq) are modeled to have less interglacial retreat (e.g. Otto-Bliesner et al., 2006)

Methods

Sampling Strategy

We analyzed three different types of samples: subglacial sediment extracted below ice boreholes, ice-bound sediment collected at the glacial margin, and glaciofluvial sediment collected from outlet streams at or near the active ice margin. Samples of subglacial sediment accessed through hot water drilling at ablation zone sites were collected in 2011 by independent drill teams working inland from Kangerlussuaq (n=2) (Graly et al., 2016) and Ilulissat (n=2) (Ryser et al., 2014). The Kangerlussuaq samples were collected by means of a downhole sampler; the Ilulissat samples were sediment that clung to the drill stem and were recovered upon its removal from the borehole.

Ice-bound sediment samples were collected in 2008 from Kangerlussuaq (n=10), Ilulissat (n=8), and Upernavik (n=16). At one Upernavik site, samples were collected in a vertical transect across the basal ice layer, allowing comparison of the measured isotope

data to ice depth. Ice-bound samples were removed with ice axe or chisel, stored in sealed Nasco whirlpaks, and melted in the field. In the laboratory, the meltwater was decanted, and the sediment dried. The ice-bound and subglacial samples were not sorted by grain size but are predominately fine sand and silt (Graly et al., 2016).

Nine samples of outlet stream glaciofluvial sediment were collected in 2011 and 2012 from Narsarsuaq (n=2), Tasiilaq (n=2), and Kangerlussuaq (n=5). The glaciofluvial samples have been previously analyzed for *in situ* ^{10}Be and, in some cases, ^{26}Al (Bierman et al., 2016; Nelson et al., 2014). The glaciofluvial samples were taken from the 250-800 µm grain size fraction, in which *in situ* ^{10}Be and ^{26}Al were also measured (Nelson et al., 2014).

Stable Isotopes

We measured $\delta^{18}O$ in the meltwater from the ice-bound samples using equilibration with CO_2 gas (Socki et al., 1992), and measured $\delta^{2}H$ using H_2 extraction by elemental zinc (Coleman et al., 1982). Results are reported using the standard delta (δ) notation, in units of ‰ relative to Vienna Standard Mean Ocean Water (VSMOW). Organic carbon (C) and total nitrogen (TN) were analyzed by combusting sediment in sealed tin capsules and analyzing the gas released in a CE Instruments NC 2500 elemental analyzer calibrated with OAS B-2152 (1.65% ± 0.02 C, 0.14% ± 0.01 N) and OAS B- 2150 (6.72%±0.17 C, 0.50%±0.01 N) standards and using Eager 200 data handling software. The precision of the analyzer is ~1% of the quantity measured for C, and ~0.5% for TN.

^{10}Be measurements

Meteoric ^{10}Be was isolated using total fusion of sediment pulverized to fine silt, in a modification of the KHF_2 flux method (Stone, 1998); the ice-bound samples were extracted in 2009 and measured in 2010; the glaciofluvial and drill samples were extracted and measured in 2017. We added ~300 μg ^{9}Be as a carrier (Tables 1 and 2). The $^{10}Be/^{9}Be$ ratio was measured by accelerator mass spectrometry at Lawrence Livermore National Laboratory and referenced to primary standard 07KNSTD3110, with an assumed $^{10}Be/^{9}Be$ ratio of $2.85 \cdot 10^{-12}$ (Nishiizumi et al., 2007). A full process blank was measured with each batch of 16 samples. The $^{10}Be/^{9}Be$ of processed blanks was $1.51 \cdot 10^{-14} \pm 1.22 \cdot 10^{-15}$ for the samples measured in 2010 (n = 3, average, 1SD) and $2.55 \cdot 10^{-14} \pm 1.06 \cdot 10^{-15}$ for the samples in 2017 (n = 1). However, in the batch of samples processed in 2017 (Table 2), five sample had values below detection limits, have their measured ratios either similar to or less than the blank. Therefore, to make a blank correction to the other measured ratios in the batch we used an average of the blank ratio and those of these five samples. In both cases, we subtracted the average ratio representative of the blank and propagated uncertainties in quadrature.

Transport time estimates

At the locations where we sampled ice-bound sediment, we estimated transport rates along the associated modern flowlines. The estimates are based on two dimensional geophysical reconstructions of the modern flowlines (Wang et al., 2002) in which each flowline is derived from 1 km horizontal grid components and 100 vertical layers. Given that the reconstructed vertical velocity is small compared to the horizontal velocity, only the horizontal velocity was used to determine transport times. The total time required to

transport sediment from a position in the interior to the margin was calculated by summing the inverse of the horizontal flow rates for the basal ice layer along these flowlines. As noted above, this approach neglects the time the sediment may spend sequestered with other basal material due to the cycling of sediment between the bed and the overlying ice. As such, transport times are likely minima.

Statistical Methods

To compare meteoric ^{10}Be data between sites and sampling techniques, we determined statistical significance through an unequal-variance, two-tailed, log-normal t-test. We used a maximum likelihood estimation to constrain the maximum $^{10}Be_{met}$ concentration in ice-bound sediment at each of our sites. We did not attempt to constrain this value for glaciofluvial sediment or subglacial sediment, as the sample size was much smaller. We considered the ice-bound samples to be discrete and random samples of the underlying sediment. Assuming a log-uniform distribution of $^{10}Be_{met}$ concentration within a soil profile, the maximum likelihood estimator of the maximum is the observed value (Ruggles and Brodie, 1947). An unbiased estimate of the maximum was calculated via:

$$M_{ub} = e^{\log M + \frac{\log M - \log m}{k-1}} \quad (2)$$

where M_{ub} is the unbiased estimate of the maximum, M is the observed maximum, m is the observed minimum, and k is sample size. Uncertainty was calculated as the difference between the unbiased (M_{ub}) and maximum likelihood (M) estimates.

To estimate the $^{10}Be_{met}$ inventory of the source soils from our estimates of the soil maximum $^{10}Be_{met}$ concentration, we employed the correlation between maximum $^{10}Be_{met}$ soil concentration and total $^{10}Be_{met}$ inventory following Graly and others (2010). Though

the correlation curve of Graly and others (2010) was constructed using primarily mid-latitude soils, we added recent measurements from arctic soils in Sweden (67˚ N) (Ebert et al., 2012) and Alaska (70˚N) (Bierman et al., 2014). Errors were propagated from both the maximum concentration estimate and the correlation with inventory to establish uncertainty in the $^{10}Be_{met}$ inventory of the sources for ice-bound sediment. As past integlacial $^{10}Be_{met}$ fluxes to Greenland have only been assessed at a few, primarily Holocene locations (Sturevik-Storm et al., 2014), there is insufficient information to assign an uncertainty to past interglacial or preglacial deposition rates. So, we used the average value from mid-Holocene sections of the GISP2 core. Only uncertainty in the value of the inventory (N) was propagated through equation 1 to solve for exposure time (t). Because the maximum-inventory correlation was developed on continuously exposed soils, decay during burial can result in an overestimate of the $^{10}Be_{met}$ soil inventory. In determining whether $^{10}Be_{met}$ concentrations could have formed during the interglacial periods of the past 500,000 years, the effect of decay is inconsequential compared with other uncertainties.

Results

Measured meteoric ^{10}Be concentrations (n=48) vary from $<10^6$ to $2.1 \cdot 10^8$ atoms$\cdot$g^{-1} (Figure 3, Tables 1 and 2). Unequal variance t-tests show that ice-bound sediment contains significantly more $^{10}Be_{met}$ than glaciofluvial sediment (Table 3). Significant differences between ice-bound and glaciofluvial sediment are also found at Kangerlussuaq alone, where both types of sediment were collected (Figure 3, Table 3). The glaciofluvial $^{10}Be_{met}$ concentrations are significantly lower in Kangerlussuaq than at Narsarsuaq and Tasiilaq, and the ice-bound $^{10}Be_{met}$ concentrations are significantly lower at Kangerlussuaq

than at Upernavik and Ilulissat. Samples from Upernavik and Ilulissat are not statistically distinguishable from each other; nor are samples from Tasiilaq and Narsarsuaq (though n=2 at these sites). The ice-bound sediment at the GISP2 base (Bierman et al., 2014) is significantly enriched in $^{10}Be_{met}$ compared to any of the marginal sites (Figure 3, Table 3).

In the ice-bound samples, the $\delta^{18}O$ values of the ice range from -38.9‰ to -24.3‰; $\delta^{2}H$ values range from -273.8‰ to -195.1‰ (Table 4). Average deuterium excess is 3.1‰ (Table 4). At the Upernavik transect site, the $\delta^{2}H/\delta^{18}O$ slope is 5.85 ± 0.83 (Figure 4). At the Upernavik transect site, deuterium excess, organic C concentration, and meteoric ^{10}Be concentration are highest at top of the basal ice layer and decrease toward the bed (Figure 5).

In most (30 of 40) of the ice-bound sediment samples, organic carbon concentrations are <0.1%. The remaining samples (n=10) have organic C concentrations from 0.16% to 1.53% (Table 4). The highest measured $^{10}Be_{met}$ concentrations corresponds to the highest measured organic carbon concentration, and the two values are correlated within the Upernavik transect site (R^2 = 0.88; Figure 5). However other sites, especially Ilulissat, have considerable $^{10}Be_{met}$ concentrations (up to $1.5 \cdot 10^8$ atoms$\cdot g^{-1}$) without any detectable organic carbon. Total nitrogen content also correlates weakly (R^2 = 0.55, p=0.05) with $^{10}Be_{met}$ content across the data set (Table 3). In the 10 samples with higher organic C concentrations, the C/N ratio is 7.5 ± 2.0 (S.E.).

At each of the flowlines for which we analyzed ice-bound sediment, modeled sediment evacuation times were 10^3-10^4 years within ~100 km of the modern ice margin and increased exponentially to ~10^5 years if sediment were sourced near the continental flow divide (Figure 6).

Using Eq. 2 and the measured maximum ^{10}Be concentrations of $4.63 \cdot 10^7$, $1.46 \cdot 10^8$, and $2.08 \cdot 10^8$ atoms$\cdot g^{-1}$ at Kangerlussuaq, Ilulissat, and Upernavik, respectively, we estimate the maximum ^{10}Be concentration in a uniform source for each site is $6.50 \pm 1.90 \cdot 10^7$, $2.40 \pm 0.98 \cdot 10^8$, and $2.69 \pm 0.62 \cdot 10^8$ atoms$\cdot g^{-1}$, respectively.

The strong correlation between maximum $^{10}Be_{met}$ concentration and total soil inventory (Graly et al., 2010) allows us to infer source $^{10}Be_{met}$ inventories from the estimated maximum concentrations (Figure 7). The newly added arctic soil measurements fit well within the mid-latitude trend. Propagating uncertainty through the correlation, we infer meteoric ^{10}Be inventories in the source sediment for the ice-bound sediment at Kangerlussuaq, Ilulissat, and Upernavik of $8.17 \pm 3.46 \cdot 10^9$, $4.18 \pm 2.32 \cdot 10^{10}$, and $4.82 \pm 1.73 \cdot 10^{10}$ atoms$\cdot cm^{-2}$, respectively. If deposition rates from the mid-Holocene are taken to represent conditions during earlier interglacial periods, we infer minimum exposure times (that do not account for loss to decay during ice cover) of 90-197 ka at Upernavik, 54-195 ka at Ilulissat, and 13-34 ka at Kangerlussuaq.

Discussion

Our isotopic data lead to three principal observations: (1) The maximum observed $^{10}Be_{met}$ concentrations are comparable to those found in well-developed mid-latitude soils (Graly et al., 2010). (2) Ice-bound sediment has significantly more $^{10}Be_{met}$ than glaciofluvial samples. (3) Sediment transported by the northern outlet glaciers that drain the Greenland Ice Sheet's main dome have significantly higher $^{10}Be_{met}$ concentrations than sediment transported by ice from the ice sheet's southern dome.

Exposure time and erosion estimates for ice-bound samples

The high concentrations of $^{10}Be_{met}$ in most ice-bound sediment from Upernavik and Ilulissat likely developed over extended periods of preglacial and/or interglacial exposure. The global benthic $\delta^{18}O$ record suggests that during the past Ma, global ice volume was less than present during four brief periods: the mid-Holocene (8 ka – 3 ka), the Eemian (MIS 5e – 127 ka – 116 ka), MIS 9 (333 ka – 323 ka), and MIS 11 (417 ka – 397 ka) (Bintanja and van de Wal, 2008). Though there are uncertainties in all global sea level reconstruction approaches, independent alternate methods indicate comparably brief interglacial periods in the late Pleistocene (Rohling et al., 2010). The decay-corrected sum of these periods is equivalent to ~40 ka of continuous exposure, less than the minimum surface exposure time that we infer from $^{10}Be_{met}$ for Ilulissat of 54 ka and far less than the Upernavik minimum exposure time of 90 ka. This means that the analyzed sediment from these two sites very likely records an exposure history beyond the global ice minima of the past million years.

Though it is not possible to attribute the observed $^{10}Be_{met}$ concentrations to any particular exposure, decay, and erosion history, the long minimum exposure times we calculate suggest that some of the $^{10}Be_{met}$ in the ice-bound sediment from Ilulissat and Upernavik likely remains from preglacial soils. Alternatively, the Greenland Ice Sheet might have had substantially longer periods of interglacial exposure than suggested by global records; exposure length would have to be more than twice the global average to even reach the Upernavik minimum. Prior to glaciation, continental surfaces probably developed deep soil profiles with tens of meters of regolith (Lidmar-Bergström, 1997). The preservation of such preglacial sediment requires integrated Quaternary subglacial erosion

417 rates be <10 m·Ma^{-1} in the source regions of the ice-bound sediment at the northern sites,
418 Upernavik and Ilulissat.

419 The last sustained period when global ice volume was reduced below present levels
420 occurred ~2.7 Ma (Lisiecki and Raymo, 2005), or about two ^{10}Be half-lives ago. If the
421 meteoric ^{10}Be in the ice-bound sediment is exclusively pre-Quaternary, initial
422 concentrations in the range of 6-8·10^{8} ^{10}Be$_{met}$ atoms·g^{-1} would be required to explain the
423 current inventory, accounting for radioactive decay. If an extensive ice-free period formed
424 much of the initial ^{10}Be$_{met}$ inventory during the early or mid-Pleistocene (i.e. Funder et al.,
425 2001; Schaefer et al., 2016), then preglacial ^{10}Be$_{met}$ concentrations on the order of 3-4·10^{8}
426 ^{10}Be atoms·g^{-1} could have produced the highest concentrations we measured in the ice-
427 bound marginal sediment. In previous studies of deeply weathered soils, ^{10}Be$_{met}$
428 concentrations of the order of 3 to 8·10^{8} atoms·g^{-1} have been found only in the soil B
429 horizon (Bacon et al., 2012; Pavich et al., 1985). For a preglacial B horizon at a depth < 2
430 m to still supply sediment to the margin, subglacial erosion rates of < 1 m·Ma^{-1} are
431 necessary for the Quaternary. The record of offshore sedimentation suggests that erosion
432 rates on that order are unlikely to be widespread (Bierman et al., 2016; Laine, 1980).
433 Instead, an initial ^{10}Be inventory remaining from the development of deep preglacial
434 regolith was likely enhanced during subsequent periods of interglacial exposure (Figure 1).

435 In low erosion rate settings, a small amount of ^{10}Be$_{met}$ accumulation may also have
436 occurred from the basal melt of the overlying ice. However, the delivery rates through basal
437 melting are not sufficient to account for the measured concentration maxima. The flux rate
438 from basal melt of 1.8·10^{4} atoms·cm^{-2}·yr^{-1} would take ~10,000 years of melt delivered to
439 a single g·cm^{-2} of sediment to obtain concentrations of 2·10^{8} atoms·g^{-1}. If the ^{10}Be$_{met}$ were

vertically distributed as it is in a typical terrestrial soil profile, with the isotope distributed over several m of depth, hundreds of thousands of years of melt are needed to reach even the concentrations found at Kangerlussuaq. However, if the subglacial sediment cover is thin (i.e. a few cm) or $^{10}Be_{met}$ is not downwardly mobile within a sediment column, a substantial portion of the meteoric ^{10}Be concentration could come from subglacial melting. Therefore, we cannot rule out some $^{10}Be_{met}$ contribution from sub-glacial melt; though, it likely represents a small fraction of the total inventory.

The long potential transport times for ice-bound sediment in the ice sheet basal layer may play a role in the preservation of sediment with a history of preglacial and interglacial exposure. Regardless of erosion rate, mid-Holocene sediment from near the margin and Eemian (MIS 5e) sediment from the interior could still be emerging at the margin as ice-bound sediment due to the slow rate of ice transport (Figure 6). The idea that older sediment may source from deeper in the interior of the ice sheet is further supported by the vertical transect collected at Upernavik (Figure 5). We expect that basal ice layers grow progressively from the bed, with the top of the layer containing sediment that was entrained earliest (Rempel, 2008). At the Upernavik vertical transect, the highest $^{10}Be_{met}$ concentrations and organic C concentrations are found at the top of the transect, suggesting a source of preglacial regolith and/or lower erosion rates deeper in the interior compared to a more marginal source for the stratigraphically lower samples.

The water stable isotope values of the ice-bound samples also suggest multiple entrainment events in the formation of the basal ice layers. The slope of stable isotope enrichment at the Upernavik vertical transect (Figure 4) is consistent with isotopic enrichment during open-system regelation, which should be approximately 5.5 for ice of

this isotopic composition (Jouzel and Souchez, 1982; Lehmann and Siegenthaler, 1991). A single regelation enrichment event decreases the deuterium excess of the ice by ~3 - 7‰, depending on the proportion of the ice that melts (Jouzel and Souchez, 1982). Assuming clean glacial ice has deuterium excess near 10‰ (Dansgaard, 1964), most samples experienced multiple enrichment events (Table 4). The conclusion that basal ice layers grew progressively through multiple regelation enrichment events is consistent with a long residence time of the sediment within the upper portions of the basal ice layer.

Erosion conditions for glaciofluvial and subglacial samples

Glaciofluvial samples have significantly lower $^{10}Be_{met}$ concentrations than ice-bound sediment (Figure 3), suggesting that they are sourced from a more erosive portion of the ice sheet than the ice-bound samples. The average $^{10}Be_{met}$ concentration in the Kangerlussuaq glaciofluvial samples is ~10^6 atoms·g^{-1}, whereas the ice-bound sediment there averages $1.3 \cdot 10^7$ atoms·g^{-1}, a more than ten-fold difference.

The $^{10}Be_{met}$ concentrations in glaciofluvial sediment can be explained from meltwater-driven ^{10}Be addition alone, without any inheritance from preglacial or interglacial soil development. Assuming the surface ice and snow that feed ablation zone melt contain $^{10}Be_{met}$ concentrations of $2 \cdot 10^4$ atoms·g^{-1} (Finkel and Nishiizumi, 1997), a liter of glacial meltwater contains $2 \cdot 10^7$ atoms of $^{10}Be_{met}$. Measured concentrations of suspended sediment in Greenland Ice Sheet meltwaters range from 1 to 10 g·L^{-1} (Cowton et al., 2012; Overeem et al., 2017). If most $^{10}Be_{met}$ sorbed to sediment grain surfaces during fluvial transport (You et al., 1989), $^{10}Be_{met}$ concentrations of 10^6 to 10^7 atoms·g^{-1} could be expected in glaciofluvial sediment, simply from the mixing of sediment and surface glacial

meltwater. The glaciofluvial samples cluster toward the low end of this range, perhaps implying incomplete partitioning of the meltwater $^{10}Be_{met}$ to solids or a preference of the isotope for fine-grain size fractions underrepresented in these sand-sized samples. If the $^{10}Be_{met}$ concentrations measured in glaciofluvial sediment were derived mostly from meltwater, then these sediments are derived from material that has little or no $^{10}Be_{met}$ remaining from preglacial or interglacial periods. This implies glacial erosion sufficient to remove previously exposed sediment in the glaciofluvial sediment from Kangerlussuaq and Tassiilaq.

The glaciofluvial samples in which we measured $^{10}Be_{met}$ were previously analyzed for *in situ* cosmogenic isotopes (Nelson et al., 2014). The measured concentrations are very low for both *in situ* (10^3 atoms g^{-1}) and meteoric ^{10}Be ($< 10^6$ atoms g^{-1}) and no significant correlation between the two is observed in the samples of solely glacial origin (Table 2). The measured *in situ* concentrations do not necessarily imply surface exposure, as muons are capable of producing small quantities of ^{10}Be at up to 100 m depth (Heisinger et al., 2002; Nelson et al., 2014). We interpret the combined *in situ* and meteoric ^{10}Be data in glaciofluvial sediment as implying very little or no previous exposure of this sand-sized sediment at or near Earth's surface.

In contrast to Kangerlussuaq and Tassiaq, two fluvial samples from Narsarsuaq suggest possible preglacial or interglacial surface exposure. One sample from a non-glaciated fluvial system has a $^{10}Be_{met}$ concentration of $1.3 \cdot 10^8$ atoms$\cdot g^{-1}$ (Table 2). Due to higher precipitation than elsewhere in Greenland, the meteoric ^{10}Be deposition rate at Narsarsuaq is ~10^6 atoms$\cdot cm^{-2} \cdot a^{-1}$ (Heikkilä and Von Blanckenburg, 2015). If the measured non-glacial fluvial concentration represents the average $^{10}Be_{met}$ content of a

steadily developing soil profile, it would take 15-30 ka to develop the source soil, probably exceeding what developed in the 11 ka since deglaciation (Carlson et al., 2014). Narsarsuaq also has the highest $^{10}Be_{met}$ value we measured in a glaciofluvial sample (Table 2). These two datapoints are consistent with some preglacial or interglacial exposure preserved in the Narsarsuaq area. Comparatively large *in situ* ^{10}Be concentrations were also observed in some of the sediment from Narsarsuaq (Nelson et al., 2014). The high topographic relief in the Narsasuaq area may be a factor in preserving low erosion, highland regions capable of preserving interglacial or preglacial sediment.

The differences between the glaciofluvial samples and the ice-bound samples are very likely due to erosive power of subglacial streams, which far exceed the erosive power of ice entrainment processes (Alley et al., 1997). If sediment from low erosion rate subglacial regions (represented by ice-bound sediment samples) is present in subglacial streams, it comprises an undetectably small fraction. At Kangerlussuaq, the order of magnitude difference between ice-bound and glaciofluvial sediment requires that <10% of the ice-bound sediment could be mixed into the glaciofluvial sediment, even assuming that glaciofluvial processes introduced no $^{10}Be_{met}$ through delivery by water. It is therefore likely that the ice-bound sediment with high $^{10}Be_{met}$ concentrations is sourced from a region outside of the influence of glaciofluvial processes, either beyond the marginal region (at most, a few 10s of km wide) that supports subglacial conduits (Dow et al., 2014) or from an area disconnected from glacial hydrologic system.

The subglacial samples collected from hot water boreholes could be comparable to glaciofluvial sediment or ice-bound sediment, depending on the conditions at the bed. At Kangerlussuaq, subglacial samples collected from the ablation zone have very low $^{10}Be_{met}$

532 levels, comparable to glaciofluvial samples collected at the margin (Table 2). At Ilulissat,
533 $^{10}Be_{met}$ concentrations are comparable to the ice-bound sediment collected at the margin.
534 Both subglacial sampling sites are located within the ablation zone, near where moulins
535 actively contact the bed (Andrews et al., 2014). This could imply that, at least at Ilulissat,
536 spatial heterogeneity in the glaciohydrological system permits low erosion zones to exist
537 in the ablation zone.
538
539 *Context of Greenland erosion and sediment flux*
540 Proglacial regions with erosion rates low enough to preserve rock surfaces over
541 multiple glacial cycles are observed in several marginal regions of Greenland, including
542 Thule (Corbett et al., 2016), Upernavik (Corbett et al., 2013), Jameson Land (Håkansson
543 et al., 2008), and Sukkertoppen (Beel et al., 2016). Similar regions under the ice may be
544 the source of the ice-bound and subglacial sediment with high $^{10}Be_{met}$ concentrations.
545 However, ice-bound sediment like those we measured still must have been subjected to
546 warm-based subglacial processes in order to become entrained and transported to the ice
547 margin, whereas currently proglacial regions could have been cold-based, and therefore
548 non-erosive, for their entire glacial histories.
549 The large difference in $^{10}Be_{met}$ concentrations between glaciofluvial and ice-bound
550 samples at Kangerlussuaq mirrors large differences in contemporary sediment fluxes from
551 the region. Contemporary ice-bound sediment fluxes in the Kangerlussuaq area are ~20
552 $m^3 \cdot m^{-1} \cdot a^{-1}$ (Knight et al., 2002), suggesting an average of ~40 $m \cdot Ma^{-1}$ of subglacial erosion
553 over the 340 km flowline (assuming rock is 50% denser than sediment). Erosion rates
554 calculated from glaciofluvial sediment flux at the Leverett Glacier (also in the

555 Kangerlussuaq area) are on the order of 1000 m·Ma^{-1} (Cowton et al., 2012), sufficient to
556 strip the evidence of even a mid-Holocene interglacial exposure. Contemporary sediment
557 fluxes in the Kangerlussuaq area are among the highest observed in Greenland (Overeem
558 et al., 2017), although contemporary sediment flux data are not necessarily representative
559 of the long-term. Such sediment flux rates are consistent with ice-bound sediment sourcing
560 from material capable of preserving a memory of interglacial exposure and glaciofluvial
561 sediment sourcing from material where erosion rates are too high to maintain this memory.
562 The long residence time of ice-bound sediment may also play a role in preserving an
563 exposure signal in $^{10}Be_{met}$ concentrations (i.e., Figure 6).

564 The thicknesses of glacial sediment as measured by offshore cores generally
565 suggest far lower long-term erosion rates than the contemporary fluxes observed at
566 Kangerlussuaq. Several cores in the Disko Bugt region (near Ilulissat) have background
567 sedimentation rates around 100 m·Ma^{-1} that spike to ~2,000 m·Ma^{-1} during periods of
568 deglaciation (Cofaigh et al., 2013). If the regions of erosion and deposition are equal in
569 area, the background sedimentation rate is equivalent to 50 m·Ma^{-1} of subglacial erosion
570 (though the channeling of ice into distinct outlets implies that the true value is lower).
571 Analysis of authigenic $^{10}Be/^{9}Be$ in a sediment core from the center of Baffin Bay suggests
572 slightly higher erosion rates for the entire region, with background rates near 80 m·Ma^{-1}
573 that approximately double during Heinrich events (Simon et al., 2016). Rates of sediment
574 deposition in the near shelf of central East Greenland are similar to those measured in West
575 Greenland, though deposition rates in fjords are an order of magnitude higher (Andrews et
576 al., 1994). Andrews and others (1994) suggest these sedimentation rates imply Holocene
577 erosion on the order of 10 m·Ma^{-1}. If erosion rates between 10-50 m·Ma^{-1} are taken as

typical, the variation between high and low erosion regions suggest Quaternary erosion rates on the order of 5-10 $m \cdot Ma^{-1}$ are plausible for portions of the subglacial environment.

The existence of glaciofluvial outlet systems capable of performing most of the erosion and sediment transport to the shelf may explain the differences in *in situ* cosmogenic isotopes observed in Greenland's onshore (Schaefer et al., 2016) and offshore (Bierman et al., 2016) records. The lack of evidence for surface exposure during the past 1.8 Ma in marine sediment cores (Bierman et al., 2016) may be in part because the vast majority of the sediment comes from subglacial streams too erosive to preserve an interglacial exposure record. However, the more minimally erosive regions of the ice sheet, both preserved in central Greenland at the base of the GISP2 ice core (Bierman et al., 2014; Schaefer et al., 2016) and at the marginal sites presented here, do contain a record of extensive pre-glacial or interglacial exposure.

The southwest region of the Greenland ice sheet, where Kangerlussuaq is located, has been modeled by many as the ice sheet's most responsive sector to changing climate (Helsen et al., 2013; Stone et al., 2013). The source regions for Kangerlussuaq's marginal sediment likely had more total exposure than any other site, and yet have significantly less $^{10}Be_{met}$. Upernavik, by contrast, is located in one of the most stable sectors of the ice sheet (Otto-Bliesner et al., 2006) and yet has the highest $^{10}Be_{met}$ observed in marginal sediment. Sediment from the stable center of Greenland has higher concentrations still (Bierman et al., 2014) (Figure 3). Differences in $^{10}Be_{met}$ concentrations between sites appear to be primarily controlled by erosion rates and not necessarily duration of interglacial exposure.

Conclusions

We measured $^{10}Be_{met}$ in ice-bound, glaciofluvial, and subglacial sediment collected from five marginal Greenland Ice Sheet sites. In the ice-bound sediment at the two northernmost sites, we found maximum $^{10}Be_{met}$ concentrations that are comparable to those measured in well-developed soils, evidence that these sediments were subject to 10^4 to $>10^5$ years of interglacial and preglacial exposure. Glaciofluvial sediment has very low $^{10}Be_{met}$ concentrations and do not preserve a signal of past interglacial or preglacial exposure. One site, Kangerlussuaq in central west Greenland, has significantly lower $^{10}Be_{met}$ concentrations for all sample types. Because this site has both unusually high sediment flux and a history of substantial interglacial ice retreat, it implies erosion is more influential than exposure in controlling $^{10}Be_{met}$ flux to the ice margin in sediment. Variation in subglacial processes (particularly regelation entrainment vs. glaciofluvial entrainment of sediment) causes erosion rates to vary across the subglacial landscape. Erosion rates low enough to preserve preglacial material may be confined to regions of the ice sheet that are lacking widespread influence of glaciofluvial processes.

Acknowledgements

This work was supported by funding from U.S. National Science Foundation grants ARC-071956 and ARC-1023191. Subglacial samples from Kangerlussuaq were collected with assistance from N. Humphrey and J. Harper. Drill-tip samples from the Ilulissat area were collected by L. Andrews, M. Hoffman, and M. Lüthi. Accelerator Mass Spectroscopy was performed by R. Finkel, A. Hidy, and S. Zimmerman. Three anonymous reviews and editorial handling by N. Glasser greatly improved the manuscript.

References Cited

Alley, R.B., Cuffey, K.M., Evenson, E.B., Strasser, J.C., Lawson, D.E. and Larson, G.J. (1997) How glaciers entrain and transport basal sediment: physical constraints. Quaternary Science Reviews 16, 1017-1038.

Alley, R.B., Lawson, D.E., Evenson, E.B., Strasser, J.C. and Larson, G.J. (1998) Glaciohydraulic supercooling: a freeze-on mechanism to create stratified, debris-rich basal ice: II Theory. Journal of Glaciology 44, 563-569.

Andrews, J.T., Millman, J.D., Jennings, A.E., Rynes, N. and Dwyer, J. (1994) Sediment Thickness of Holocene Glacial Marine Sedimentation Rates in Three East Greenland Fjords (ca. 68°N). Journal of Geology 102, 669-683.

Andrews, L.C., Catania, G.A., Hoffman, M.J., Gulley, J.D., Lüthi, M.P., Ryser, C., Hawley, R.L. and Neumann, T.A. (2014) Direct observations of evolving subglacial drainage beneath the Greenland Ice Sheet. Nature 514, 80.

Bacon, A.R., Bierman, P.R. and Rood, D.H. (2012) Coupling meteoric 10Be with pedogenic losses of 9Be to improve soil residence time estimates on an ancient North American interfluve. Geology 40, 847-850.

Barg, E., Lal, D., Pavich, M.J., Caffee, M.W. and Southon, J.R. (1997) Beryllium geochemistry in soils; evaluation of $^{10}Be/^{9}Be$ ratios in authigenic minerals as a basis for age models. Chemical Geology 140, 237-258.

Barjes, N.H. (1996) Total carbon and nitrogen in the soils of the world European Journal of Soil Science 47, 151-163.

Baumgartner, S., Beer, J., Wagner, G., Kubik, P., Suter, M., Raisbeck, G.M. and Yiou, F. (1997) ^{10}Be and dust. Nuclear Instruments and Methods in Physics Research B 123, 296-301.

Beel, C.R., Lifton, N.A., Briner, J.P. and Goehring, B.M. (2016) Quaternary evolution and ice sheet history of contrasting landscapes in Uummannaq and Sukkertoppen, western Greenland. Quaternary Science Reviews 149, 248-258.

Bierman, P.R., Corbett, L.B., Graly, J.A., Neumann, T.A., Lini, A., Crosby, B. and Rood, D.H. (2014) Preservation of a pre-glacial landscape under the center of the Greenland Ice Sheet. Science 344, 402-405.

Bierman, P.R., Marsella, K.A., Patterson, C., Davis, P.T. and Caffee, M. (1999) Mid-Pleistocene cosmogenic minimum-age limits for pre-Wisconsinan glacial surfaces in southwestern Minnesota and southern Baffin Island: a multiple nuclide approach. Geomorphology 27, 25-39.

Bierman, P.R., Shakun, J.D., Corbett, L.B., Zimmerman, S.R. and Rood, D.H. (2016) A persistent and dynamic East Greenland Ice Sheet over the past 7.5 million years. Nature 540, 256-260s.

Bintanja, R. and van de Wal, R.S.W. (2008) North American ice-sheet dynamics and the onset of the 100,000-year glacial cycles. Nature 454, 869-872.

Brown, L., Pavich, M.J., Hickman, R.E., Klein, J. and Middleton, R. (1988) Erosion of the eastern United States observed with ^{10}Be. Earth Surface Processes and Landforms 13, 441-457.

Carlson, A.E., Winsor, K., Ullman, D.J., Brook, E.J., Rood, D.H., Axford, Y., LeGrande, A.N., Anslow, F.S. and Sinclair, G. (2014) Earliest Holocene south Greenland ice sheet retreat within its late Holocene extent. Geophysical Research Letters 41.

Chandler, D.M., Wadham, J.L., Lis, G.P., Cowton, T., Sole, A., Bartholomew, I., Telling, J., Nienow, P., Bagshaw, E.B., Mair, D., Vinen, S. and Hubbard, A. (2013) Evolution of the subglacial drainage system beneath the Greenland Ice Sheet revealed by tracers. Nature Geoscience 6, 195-198.

Cofaigh, C.Ó., Dowdeswell, J., Jennings, A., Hogan, K., Kilfeather, A., Hiemstra, J., Noormets, R., Evans, J., McCarthy, D. and Andrews, J. (2013) An extensive and dynamic ice sheet on the West Greenland shelf during the last glacial cycle. Geology 41, 219-222.

Coleman, M.L., Shepherd, T.J., Durham, J.J., Rouse, J.E. and Moore, G.R. (1982) Reduction of water with zinc for hydrogen isotope analysis. Analytical Chemistry 54, 993-995.

Corbett, L.B., Bierman, P.R., Graly, J.A., Neumann, T.A. and Rood, D.H. (2013) Constraining landscape history and glacial erosivity using paired cosmogenic nuclides in Upernavik, northwest Greenland. Geological Society of America Bulletin 125, 1539-1553.

Corbett, L.B., Bierman, P.R. and Rood, D.H. (2016) Constraining multi-stage exposure-burial scenarios for boulders preserved beneath cold-based glacial ice in Thule, northwest Greenland. Earth and Planetary Science Letters 440, 147-157.

Corbett, L.B., Young, N.E., Bierman, P.R., Briner, J.P., Neumann, T.A., Rood, D.H. and Graly, J.A. (2011) Paired bedrock and boulder 10Be concentrations resulting from early Holocene ice retreat near Jakobshavn Isfjord, western Greenland. Quaternary Science Reviews 30, 1739-1749.

Cowton, T., Nienow, P., Bartholomew, I., Sole, A. and Mair, D. (2012) Rapid erosion beneath the Greenland ice sheet. Geology 40, 343-346.

Craig, H. (1961) Isotopic variations in meteoric water. Science 133, 1702-1703.

Dansgaard, W. (1964) Stable isotopes in precipitation. Tellus 16, 436-468.

Dow, C.F., Kulessa, B., Rutt, I.C., Doyle, S.H. and Hubbard, A. (2014) Upper bounds on subglacial channel development for interior regions of the Greenland Ice Sheet. Journal of Glaciology 60, 1044-1052.

Dowdeswell, J.A., Hogan, K.A., Cofaigh, C.Ó., Fugelli, E.M.G., Evans, J. and Noormets, R. (2014) Late Quaternary ice flow in a West Greenland fjord and cross-shelf trough system: submarine landforms from Rink Isbrae to Uummannaq shelf and slope. Quaternary Science Reviews 92, 292-309.

Ebert, K., Willenbring, J., Norton, K.P., Hall, A. and Hättestrand, C. (2012) Meteoric ^{10}Be concentrations from saprolite and till in northern Sweden: Implications for glacial erosion and age. Quaternary Geochronology 12, 11-22.

Finkel, R.C. and Nishiizumi, K. (1997) Beryllium 10 concentrations in the Greenland Ice Sheet Project 2 ice core from 3-40 ka. Journal of Geophysical Research 102, 26699-26706.

Funder, S., Bennike, O., Böcher, J., Israelson, C., Petersen, K.S. and Simonarson, L.A. (2001) Late Pliocene Greenland - The Kap København Formation in North Greenland. Bulletin of the Geological Society of Denmark 48, 117-134.

Goelzer, H., Huybrechts, P., Fürst, J.J., Nick, F.M., Andersen, M.L., Edwards, T.L., Fettweis, X., Payne, A.J. and Shannon, S. (2013) Sensitivity of Greenland ice sheet projections to model formulations. Journal of Glaciology 59, 733-749.

715 Graly, J.A., Bierman, P.R., Reusser, L.J. and Pavich, M.J. (2010) Meteoric ^{10}Be in soil
716 profiles – a global meta-analysis. Geochimica et Cosmochimica Acta 74, 6814-
717 6829.
718 Graly, J.A., Humphrey, N.F. and Harper, J.T. (2016) Chemical depletion of sediment
719 under the Greenland Ice Sheet. Earth Surface Processes and Landforms 41, 1922-
720 1936.
721 Graly, J.A., Reusser, L.J. and Bierman, P.R. (2011) Short and long-term delivery rates of
722 meteoric ^{10}Be to terrestrial soils. Earth and Planetary Science Letters 302, 329-
723 336.
724 Grant, K., Rohling, E., Ramsey, C.B., Cheng, H., Edwards, R., Florindo, F., Heslop, D.,
725 Marra, F., Roberts, A. and Tamisiea, M.E. (2014) Sea-level variability over five
726 glacial cycles. Nature communications 5, 5076.
727 Greve, R. (2005) Relation of measured basal temperatures and the spatial distribution of
728 geothermal heat flux for the Greenland ice sheet. Annals of Glaciology 42, 424-
729 432.
730 Håkansson, L., Alexanderson, H., Hjort, C., Möller, P., Briner, J.P., Aldahan, A. and
731 Possnert, G. (2008) Late Pleistocene glacial history of Jameson Land, central East
732 Greenland, derived from cosmogenic ^{10}Be and ^{26}Al exposure dating. Boreas 38,
733 244-260.
734 Hallet, B., Hunter, L. and Bogen, J. (1996) Rates of erosion and sediment evacuation by
735 glaciers: A review of field data and their implications. Global and Planetary
736 Change 12, 213-235.
737 Harden, J.W., Fries, T.L. and Pavich, M.J. (2002) Cycling of Beryllium and Carbon
738 through hillslope soils in Iowa. Biogeochemistry 60, 317-336.
739 Heikkilä, U., Beer, J. and Feichter, J. (2008) Modeling cosmogenic radionuclides ^{10}Be
740 and ^{7}Be during the Meander Minimum using the ECHAM5-HAM General
741 Circulation Model. Atmospheric Chemistry and Physics 8, 2797-2809.
742 Heikkilä, U. and Von Blanckenburg, F. (2015) The global distribution of Holocene
743 meteoric ^{10}Be fluxes from atmospheric models. Distribution maps for terrestrial
744 Earth surface applications. GFZ Data Services.
745 Heisinger, B., Lal, D., Jull, A., Kubik, P., Ivy-Ochs, S., Neumaier, S., Knie, K., Lazarev,
746 V. and Nolte, E. (2002) Production of selected cosmogenic radionuclides by
747 muons: 1. Fast muons. Earth and Planetary Science Letters 200, 345-355.
748 Helsen, M.M., van de Berg, W.J., van de Wal, R.S.W., van den Broeke, M.R. and
749 Oerlemans, J. (2013) Coupled regional climate–ice-sheet simulation shows
750 limited Greenland ice loss during the Eemian. Climate of the Past 9, 1773-1788.
751 Hubbard, B. and Sharp, M. (1993) Weertman regelation, multiple refreezing events and
752 the isotopic evolution of the basal ice layer. Journal of Glaciology 39, 275-291.
753 Huybrechts, P. (2002) Sea-level changes at the LGM from ice-dynamic reconstructions
754 of the Greenland and Antarctic ice sheets during the glacial cycles. Quaternary
755 Science Reviews 21, 203-231.
756 Iverson, N.R. and Souchez, R. (1996) Isotopic signature of debris-rich ice formed by
757 regelation into a subglacial sediment bed. Geophysical Research Letters 23, 1151-
758 1154.

759 Joughin, I., Das, S.B., King, M.A., Smith, B.E., Howat, I.M. and Moon, T. (2008)
760 Seasonal speedup along the western flank of the Greenland Ice Sheet. Science
761 320, 781-783.
762 Joughin, I., Smith, B.E., Howat, I.M., Scambos, T. and Moon, T. (2010) Greenland flow
763 variability from ice-sheet-wide velocity mapping. Journal of Glaciology 56, 415-
764 430.
765 Jouzel, J. and Souchez, R.A. (1982) Melting-refreezing at the glacier sole and the isotopic
766 composition of the ice. Journal of Glaciology 28, 35-42.
767 Kelley, S., Briner, J. and Young, N. (2013) Rapid ice retreat in Disko Bugt supported by
768 ^{10}Be dating of the last recession of the western Greenland Ice Sheet. Quaternary
769 Science Reviews 82, 13-22.
770 Knight, P.G. (1989) Stacking of basal debris layers without bulk freezing-on: Isotopic
771 eveidence from West Greenland. Journal of Glaciology 45, 214-216.
772 Knight, P.G. (1997) The basal ice layer of glaciers and ice sheets. Quaternary Science
773 Reviews 16, 975-993.
774 Knight, P.G., Waller, R.I., Patterson, C.J., Jones, A.P. and Robinson, Z.P. (2002)
775 Discharge of debris from ice at the margin of the Greenland ice sheet. Journal of
776 Glaciology 48, 192-198.
777 Korschinek, G., Bergmaier, A., Faestermann, T., Gerstmann, U.C., Knie, K., Rugel, G.,
778 Wallner, A., Dillmann, I., Dollinger, G., von Gostomski, C.L., Kossert, K.,
779 Poutivtsev, M. and Remmert, A. (2010) A new value for the half-life of ^{10}Be by
780 heavy-ion elastic recoil detection and liquid scintillation counting. Nuclear
781 Instruments and Methods in Physics Research B 268, 187-191.
782 Laine, E.P. (1980) New evidence from beneath the Western North Atlantic for the depth
783 of glacial erosion in Greenland and North America. Quaternary Research 14, 188-
784 198.
785 Lal, D. and Peters, B. (1967) Cosmic-ray produced radioactivity on earth, Handbook of
786 Physics. Springer-Verlag, Berlin, pp. 551-612.
787 Lehmann, M. and Siegenthaler, U. (1991) Equilibrium oxygen- and hydrogen-isotope
788 fractionation between ice and water. Journal of Glaciology 37, 23-26S.
789 Levy, L.B., Kelly, M.A., Howley, J.A. and Virginia, R.A. (2012) Age of the Ørkendalen
790 moraines, Kangerlussuaq, Greenland: constraints on the extent of the
791 southwestern margin of the Greenland Ice Sheet during the Holocene. Quaternary
792 Science Reviews 52, 1-5.
793 Lidmar-Bergström, K. (1997) A long-term perspective on glacial erosion. Earth Surface
794 Processes and Landforms 22, 297-306.
795 Lisiecki, L.E. and Raymo, M.E. (2005) A Pliocene-Pleistocene stack of 57 globally
796 distributed benthic δ18O records. Paleoceanography 20, PA1003.
797 Molnar, P. (2004) Late Cenozoic increase in accumulation rates of terrestrial sediment:
798 How might climate change have affected erosion rates? Annual Review of Earth
799 and Planetary Sciences 32, 67-89.
800 Nelson, A.H., Bierman, P.R., Shakun, J.D. and Rood, D.H. (2014) Using *in situ*
801 cosmogenic ^{10}Be to identify the source of sediment leaving Greenland. Earth
802 Surface Processes and Landforms 39, 1087-1100.

Nishiizumi, K., Imamura, M., Caffee, M., Southon, J.R., Finkel, R.C. and McAninch, J. (2007) Absolute calibration of ^{10}Be standards. Nuclear Instruments and Methods in Physics Research B 258, 403-413.

Otto-Bliesner, B.L., Marshall, S.J., Overpeck, J.T., Miller, G.H. and Hu, A. (2006) Simulating arctic climate warmth and icefield retreat in the last interglacial. Science 311, 1751-1753.

Overeem, I., Hudson, B.D., Syvitski, J.P., Mikkelsen, A.B., Hasholt, B., van den Broeke, M., Noël, B. and Morlighem, M. (2017) Substantial export of suspended sediment to the global oceans from glacial erosion in Greenland. Nature Geoscience 10, ngeo3046.

Pavich, M.J., Brown, L., Harden, J.W., Klein, J. and Middleton, R. (1986) ^{10}Be distribution in soils from Merced River terraces, California. Geochimica et Cosmochimica Acta 50, 1727-1735.

Pavich, M.J., Brown, L., Klein, J. and Middleton, R. (1984) ^{10}Be accumulation in a soil chronosequence. Earth and Planetary Science Letters 68, 198-204.

Pavich, M.J., Brown, L., Valette-Silver, J.N., Klein, J. and Middleton, R. (1985) ^{10}Be analysis of a Quaternary weathering profile in the Virginia Piedmont. Geology 13, 39-41.

Pavich, M.J. and Vidic, N. (1993) Application of paleomagnetic and ^{10}Be analyses to chronostratigraphy of alpine glacio-fluvial terraces, Sava River Valley, Slovenia. Geophysical monograph 78, 263-275.

Philip, R.J. (1980) Thermal fields during regelation. Cold Regions Science and Technology 3, 193-203.

Rempel, A.W. (2008) A theory for ice-till interactions and sediment entrainment beneath glaciers. Journal of Geophysical Research 113, F01013.

Rinterknecht, V., Gorokhovich, Y., Schaefer, J. and Caffee, M. (2009) Preliminary 10Be chronology for the last deglaciation of the western margin of the Greenland Ice Sheet. Journal of Quaternary Science 24, 270-278.

Roberts, D.H., Long, A.J., Schnabel, C., Davies, B.J., Xu, S., Simpson, M.J.R. and Huybrechts, P. (2009) Ice Sheet exten and early deglacial history of the southwestern sector of the Greenland Ice Sheet. Quaternary Science Reviews 28, 2760-2773.

Roberts, D.H., Long, A.J., Schnabel, C., Freeman, S. and Simpson, M.J. (2008) The deglacial history of southeast sector of the Greenland Ice Sheet during the Last Glacial Maximum. Quaternary Science Reviews 27, 1505-1516.

Rohling, E.J., Braun, K., Grant, K., Kucera, M., Roberts, A., Siddall, M. and Trommer, G. (2010) Comparison between Holocene and Marine Isotope Stage-11 sea-level histories. Earth and Planetary Science Letters 291, 97-105.

Rohling, E.J., Hibbert, F.D., Williams, F.H., Grant, K.M., Marino, G., Foster, G.L., Hennekam, R., De Lange, G.J., Roberts, A.P. and Yu, J. (2017) Differences between the last two glacial maxima and implications for ice-sheet, δ 18 O, and sea-level reconstructions. Quaternary Science Reviews 176, 1-28.

Ruggles, R. and Brodie, H. (1947) An empirical approach to economic intelligence in world war II. Journal of the American Statistical Association 42, 72-91.

Ryser, C., Luthi, M.P., Andrews, L.C., Catania, G.A., Funk, M., Hawley, R., Hoffman, M. and Neumann, T.A. (2014) Caterpillar-like icemotion in the ablation zone of the Greenland ice sheet. Journal of Geophysical Research: Earth Surface 119.

Schaefer, J.M., Finkel, R.C., Balco, G., Alley, R.B., Caffee, M.W., Briner, J.P., Young, N.E., Gow, A.J. and Schwartz, R. (2016) Greenland was nearly ice-free for extended periods during the Pleistocene. Nature 540, 252-255.

Simon, Q., Thouveny, N., Bourles, D.L., Nuttin, L., Hillaire-Marcel, C. and St-Onge, G. (2016) Authigenic $^{10}Be/^{9}Be$ ratios and ^{10}Be-fluxes ($^{230}Th_{xs}$-normalized) in central Baffin Bay sediments during the last glacial cycle: Paleoenvironmental implications. Quaternary Science Reviews 140, 142-162.

Sjunneskog, C., Scherer, R., Aldahan, A. and Possnert, G. (2007) 10Be in glacial marine sediment of the Ross Sea, Antarctica, a potential tracer of depositional environment and sediment chronology. Nuclear Instruments and Methods in Physics Research Section B: Beam Interactions with Materials and Atoms 259, 576-583.

Socki, R.A., Karlsson, H.R. and Gibson, E.K. (1992) Extraction Technique of the Determination of Oxygen-18 In Water Preevacuated Glass Vials. Analytical Chemistry 64, 829-831.

Stone, E.J., Lunt, D.J., Annan, J.D. and Hargreaves, J.C. (2013) Quantification of the Greenland ice sheet contribution to Last Interglacial sea level rise. Climate of the Past 9, 621-639.

Stone, J. (1998) A rapid method for separation of beryllium-10 from soils and silicates. Geochimica et Cosmochimica Acta 62, 555-561.

Sturevik-Storm, A., Aldahan, A., Possnert, G., Berggren, A.-M., Muscheler, R., Dahl-Jensen, D., Vinther, B.M. and Usoskin, I. (2014) ^{10}Be climate fingerprints during the Eemian in the NEEM ice core, Greenland. Scientific reports 4.

Sugden, D.E., P. G. Knight, Livesey, N., Lorrain, R.D., Souchez, R.A., Tison, J.L. and Jouzel, J. (1987) Evidence for two zones of debris entrainment beneath the Greenland Ice Sheet. Nature 328, 238-241.

Walder, J.S. and Fowler, A. (1994) Channelized subglacial drainage over a deformable bed. Journal of Glaciology 40, 3-15.

Wang, W.L., Zwally, H.J., Abdalati, W. and Luo, S. (2002) Modeling of ice flow and internal layers along a flowline through Swiss Camp, West Greenland. Annals of Glaciology 34, 303-308.

Willerslev, E., Cappellini, E., Boomsma, W., Rasmus, N., Hebsgaard, M.B., Brand, T.B., Hofreiter, M., Bunce, M., Poinar, H.N., Dahl-Jensen, D., Johnsen, S., Steffensen, J.P., Bennike, O., Schwenninger, J.-L., Nathan, R., Armitage, S., de Hoog, C.-J., Alfimov, V., Christl, M., Beer, J., Muscheler, R., Barker, J., Sharp, M., Penkman, K.E.H., Haile, J., Taberlet, P., Gilbert, M.T.P., Casoli, A., Campani, E. and Collins, M.J. (2007) Ancient biomolecules from deep ice cores reveal a forested southern Greenland. Science 317, 112-116.

Yokoyama, Y., Anderson, J.B., Yamane, M., Simkins, L.M., Miyairi, Y., Yamazaki, T., Koizumi, M., Suga, H., Kusahara, K. and Prothro, L. (2016) Widespread collapse of the Ross Ice Shelf during the late Holocene. Proceedings of the National Academy of Sciences 113, 2354-2359.

You, C.-F., Lee, T. and Li, Y.-H. (1989) The partition of Be between soil and water. Chemical Geology 77, 105-118.
Young, N.E., Briner, J.P., Rood, D.H., Finkel, R.C., Corbett, L.B. and Bierman, P.R. (2013) Age of the Fjord Stade moraines in the Disko Bugt region, western Greenland, and the 9.3 and 8.2 ka cooling events. Quaternary Science Reviews 60, 76-90.

Figure Captions

Figure 1: Conceptual model of development of $^{10}Be_{met}$ soil profiles over glacial and interglacial conditions. A) Prior to glaciation, high concentrations and large inventories of $^{10}Be_{met}$ develop in a deep regolith layer. B) During glacial periods, upper portions of this regolith are entrained in basal ice and removed from the landscape, while remaining $^{10}Be_{met}$ is reduced by radio decay. C) During interglacial periods, sediment is again exposed to $^{10}Be_{met}$ deposition and new $^{10}Be_{met}$ is added to the previous $^{10}Be_{met}$ inventory that remains. This process of glacial-period $^{10}Be_{met}$ loss and interglacial period replenishment repeats over glacial/interglacial cycles.

Figure 2: Location maps. A) Source regions of sediment delivered to sampling regions at the modern margin of the Greenland Ice Sheet based on modeled flowlines (Wang et al., 2002) B-F) Satellite imagery (Google Earth) of our sampling locations at each site.

Figure 3: Bar and whisker plots of $^{10}Be_{met}$ concentrations across all Greenland Ice Sheet sampling sites. Boxes represent 2nd and 3rd quartiles of the data. Whiskers go to the minimum/maximum or 1.5 times the interquartile range (whichever is closer to the median). Outliers beyond the whiskers are marked with an x. Data from sediments in the GISP2 ice core (Bierman et al., 2014) are shown for comparison.

Figure 4: $\delta^{18}O$ and $\delta^{2}H$ from the Upernavik transect site. The slope is lower than the slope of meteoric water, suggesting refreezing with mass dependent fraction as meltwater is lost to the subglacial system (Sugden et al., 1987).

Figure 5: Upernavik transect site data with depth of the basal ice layer. A) $^{10}Be_{met}$ concentration, organic carbon concentration, and deuterium excess vs. transect distance. B) Image of the transect site, black arrow indicates direction of deeper basal ice, white bags are sampling locations, Bell 212 helicopter for scale.

Figure 6: Total time necessary to transport ice-bound sediment to the Greenland Ice Sheet margin from a given distance in the interior based on model results of Wang et al. (2002).

Figure 7: Derivation of $^{10}Be_{met}$ inventories in source soils from the maximum measured $^{10}Be_{met}$ concentration at each site. The relationship between maximum $^{10}Be_{met}$ concentration and total $^{10}Be_{met}$ inventory in mid latitude and arctic soils is used as a calibration. Mid latitude data are from Graly et al. (2010); Alaska data are from Bierman et al. (2014); Sweden data are from Ebert et al. (2012).

Table Captions

Table 1. $^{10}Be_{met}$ data for Greenlandic Ice-bound Samples (analyzed 2010)

Table 2. $^{10}Be_{met}$ data for Greenlandic Glaciofluvial and Subglacial Samples (analyzed 2017)

Table 3. P values for two tailed t-test of log-normal distributions of various subsets of the $^{10}Be_{met}$ data. P-values <0.05 are bold.

Table 4. Stable Isotope and C/N Data

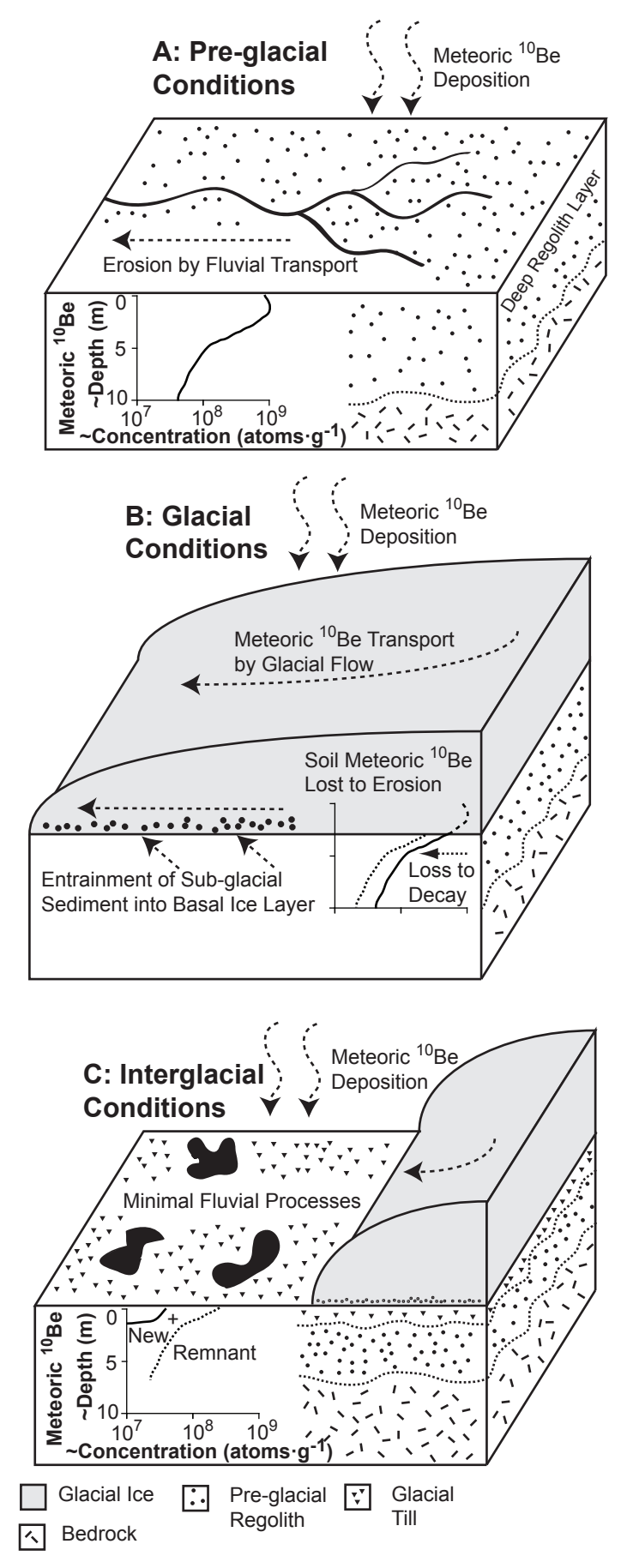
A: Pre-glacial Conditions
Meteoric 10Be Deposition
Erosion by Fluvial Transport
Deep Regolith Layer
Meteoric 10Be ~Depth (m)
0
5
10
10^7
10^8
10^9
~Concentration (atoms·g-1)
B: Glacial Conditions
Meteoric 10Be Deposition
Meteoric 10Be Transport by Glacial Flow
Soil Meteoric 10Be Lost to Erosion
Entrainment of Sub-glacial Sediment into Basal Ice Layer
Loss to Decay
C: Interglacial Conditions
Meteoric 10Be Deposition
Minimal Fluvial Processes
New
Remnant
Meteoric 10Be ~Depth (m)
0
5
10
10^7
10^8
10^9
~Concentration (atoms·g-1)
Glacial Ice
Pre-glacial Regolith
Glacial Till
Bedrock

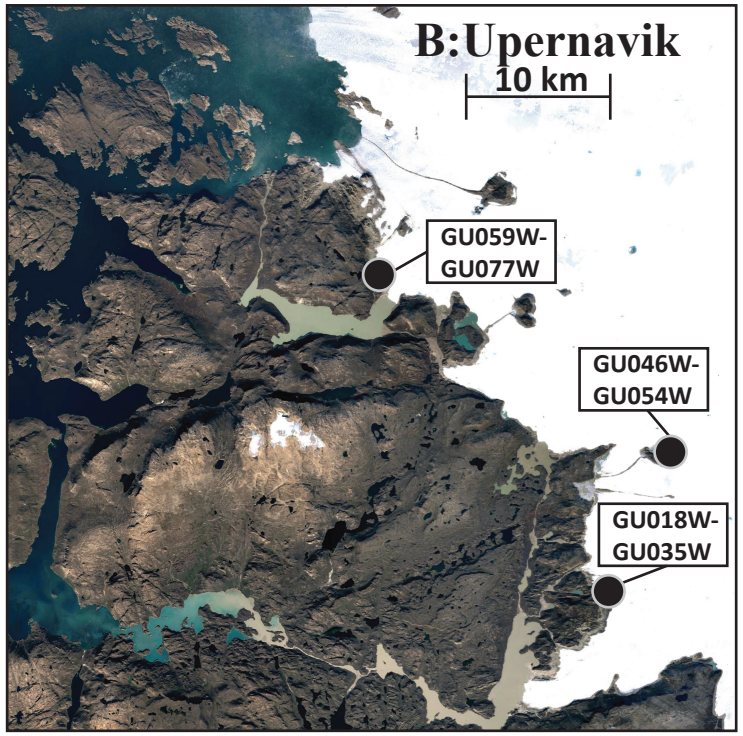

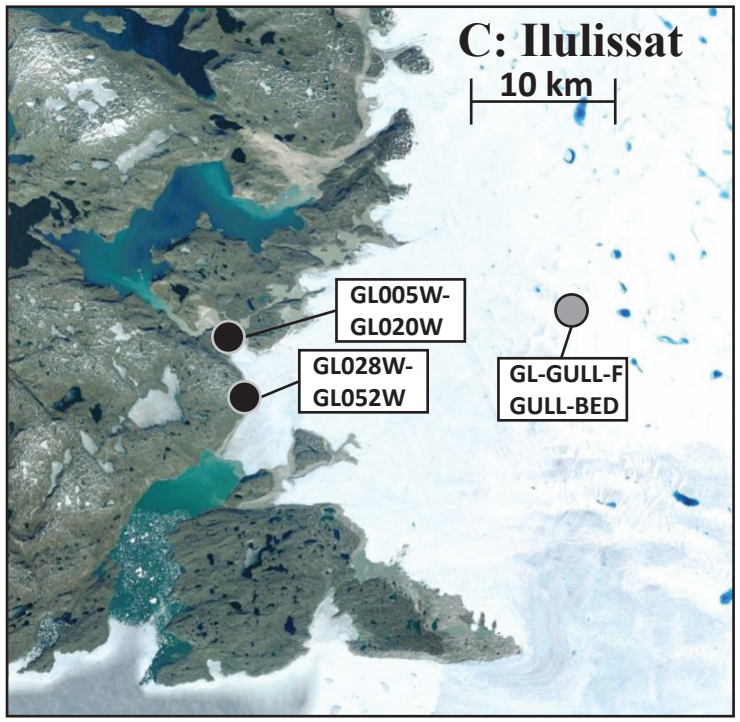

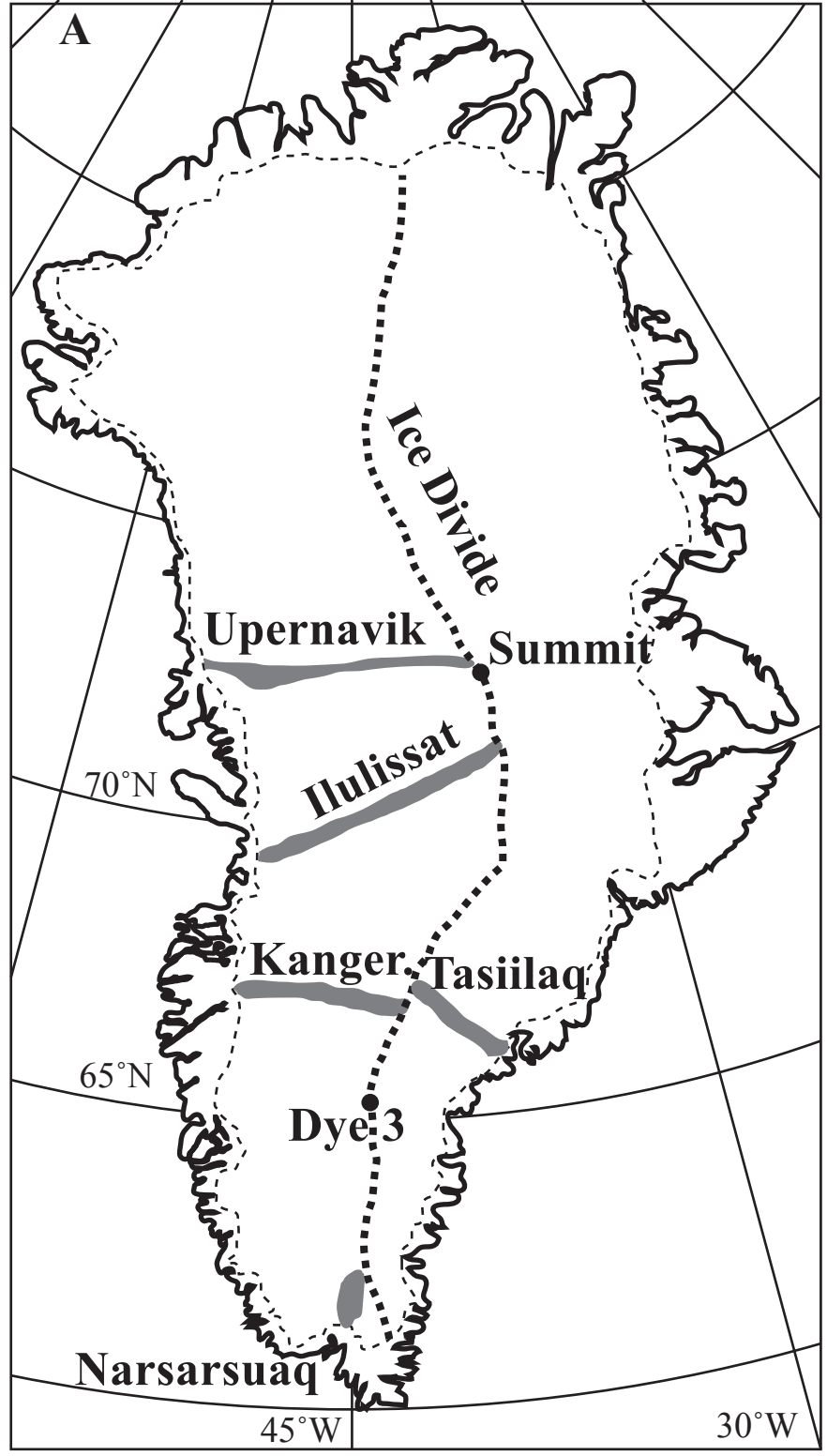

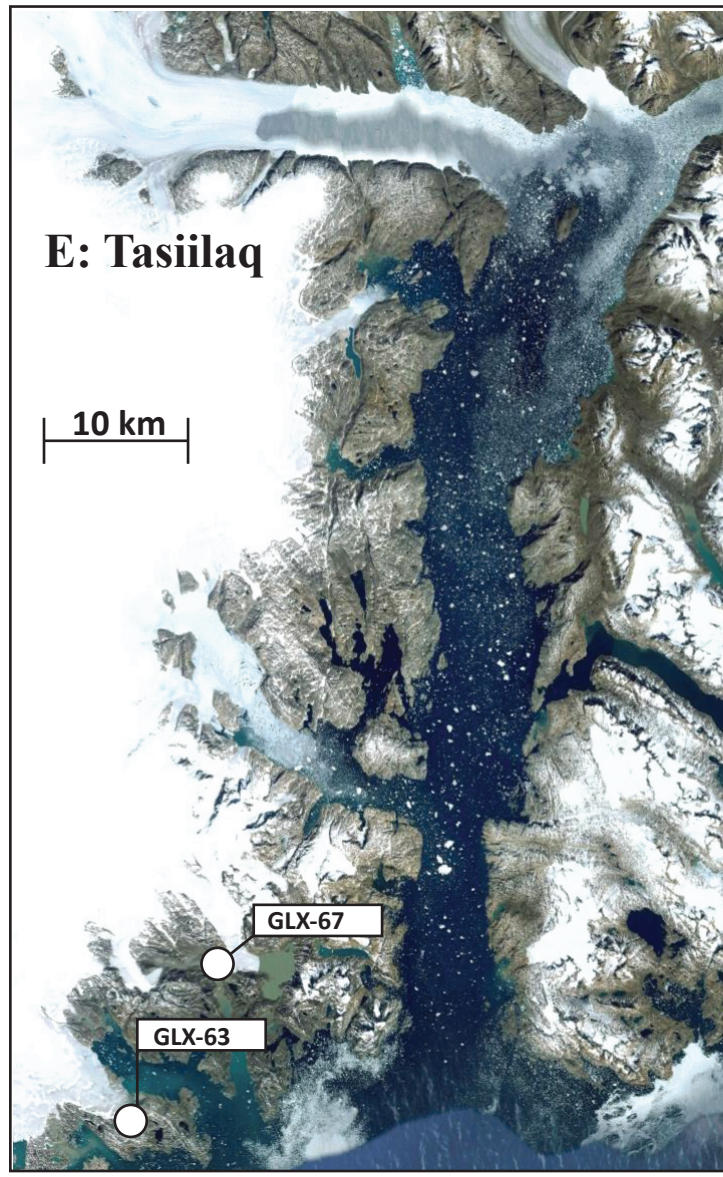

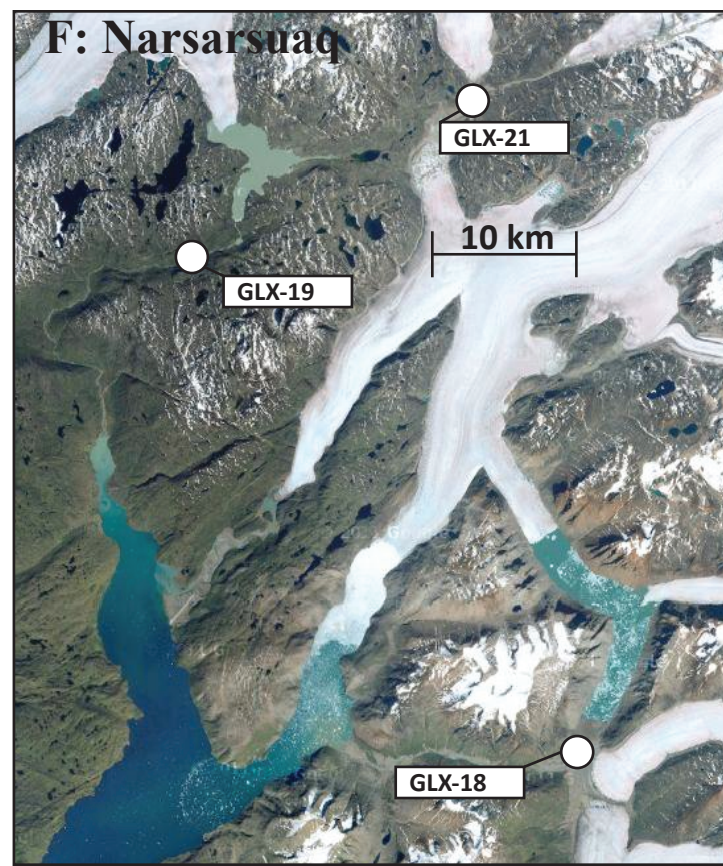

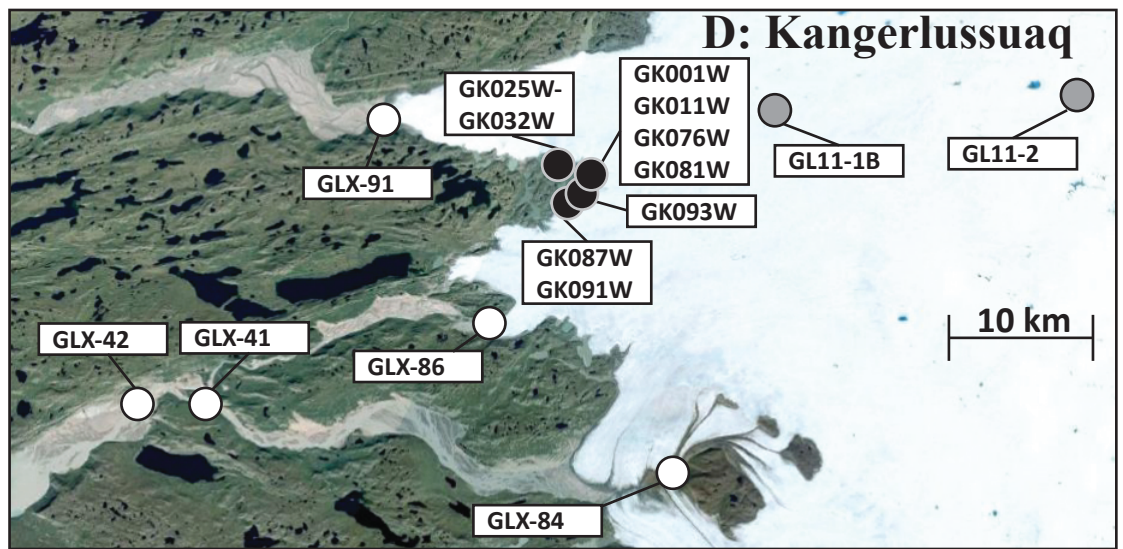

Sampling Site Type

- Ice Bound
- Glaciofluvial
- Subglacial

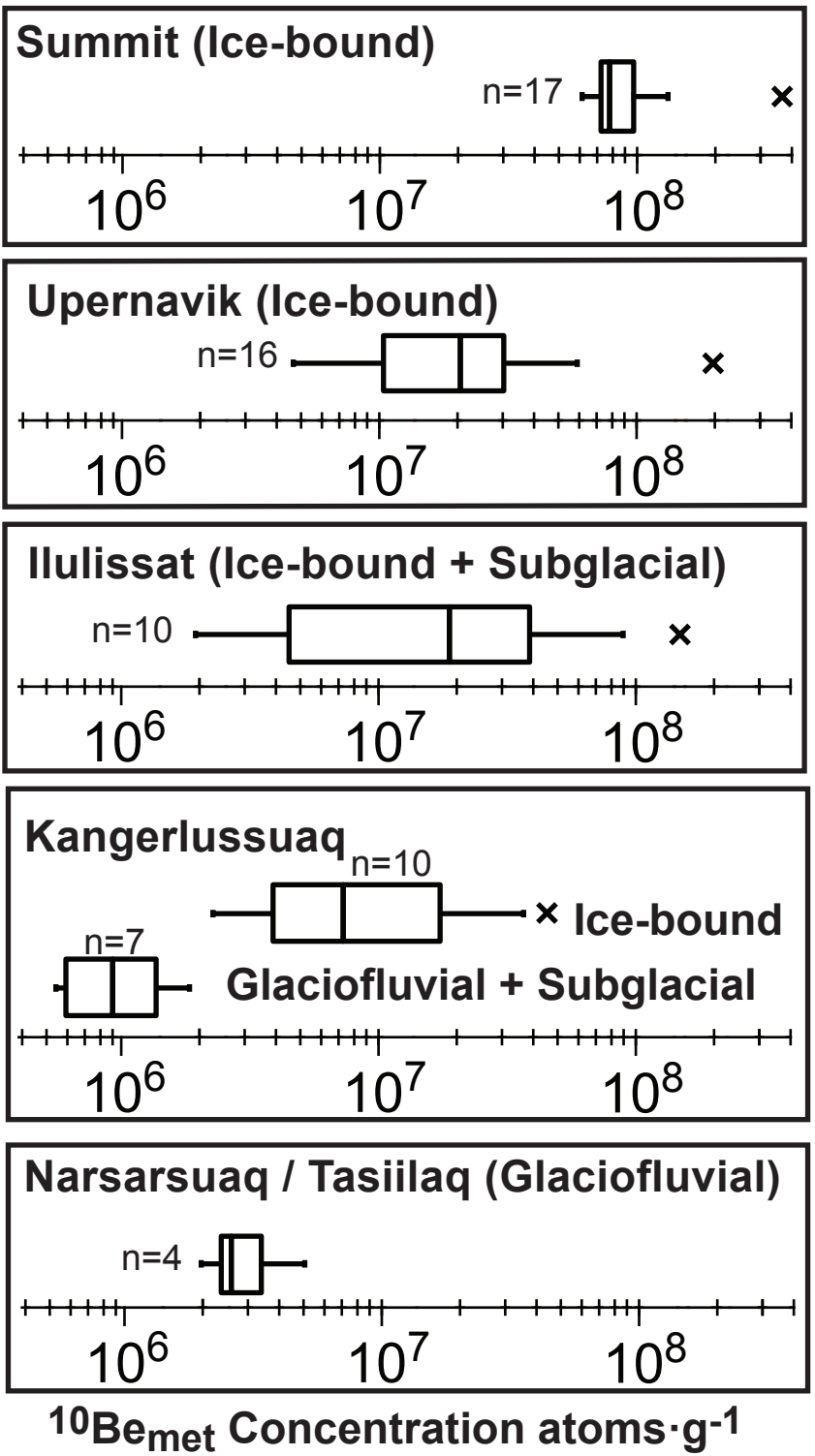
Summit (Ice-bound)
n=17
Upernavik (Ice-bound)
n=16
Ilulissat (Ice-bound + Subglacial)
n=10
Kangerlussuaq
n=10
Ice-bound
n=7
Glaciofluvial + Subglacial
Narsarsuaq / Tasiilaq (Glaciofluvial)
n=4
10^6
10^7
10^8
10Be met Concentration atoms·g-1

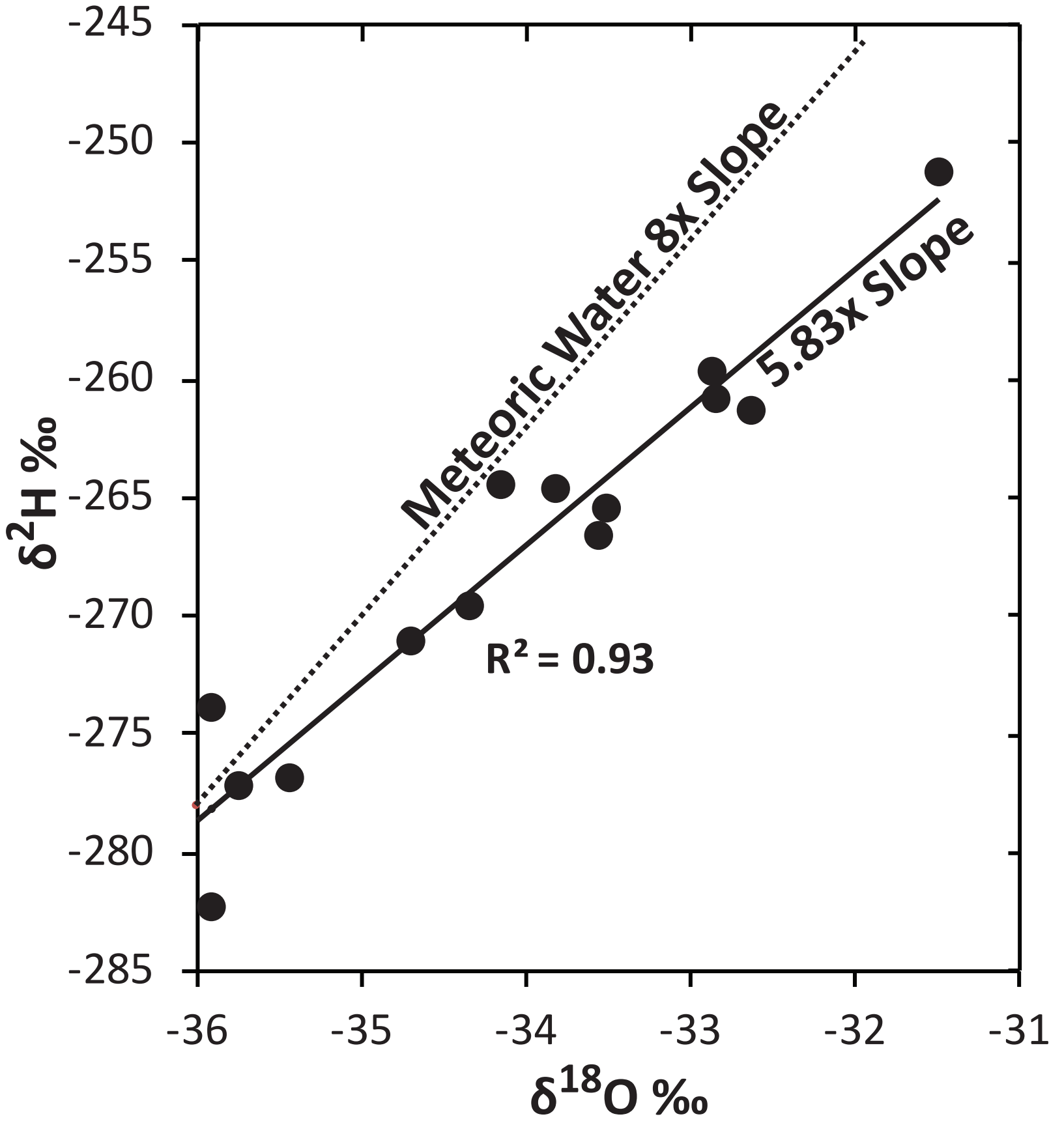
-245
-250
-255
-260
-265
-270
-275
-280
-285
-36
-35
-34
-33
-32
-31
δ2H ‰
δ18O ‰
Meteoric Water 8x Slope
5.83x Slope
R² = 0.93

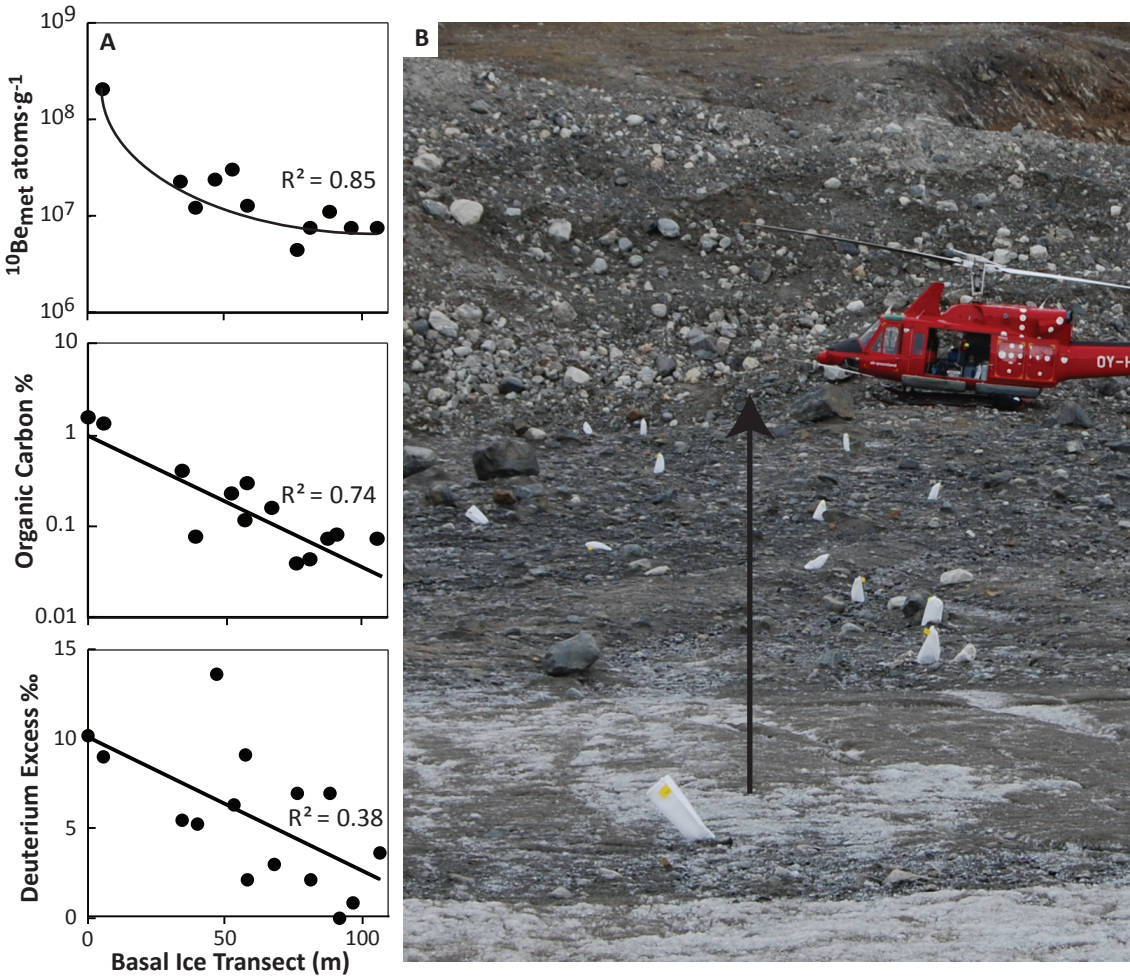
A
B
$^{10}Be_{met}$ atoms·g^{-1}
10^9
10^8
10^7
10^6
R^2 = 0.85
Organic Carbon %
10
1
0.1
0.01
R^2 = 0.74
Deuterium Excess ‰
15
10
5
0
R^2 = 0.38
0
50
100
Basal Ice Transect (m)

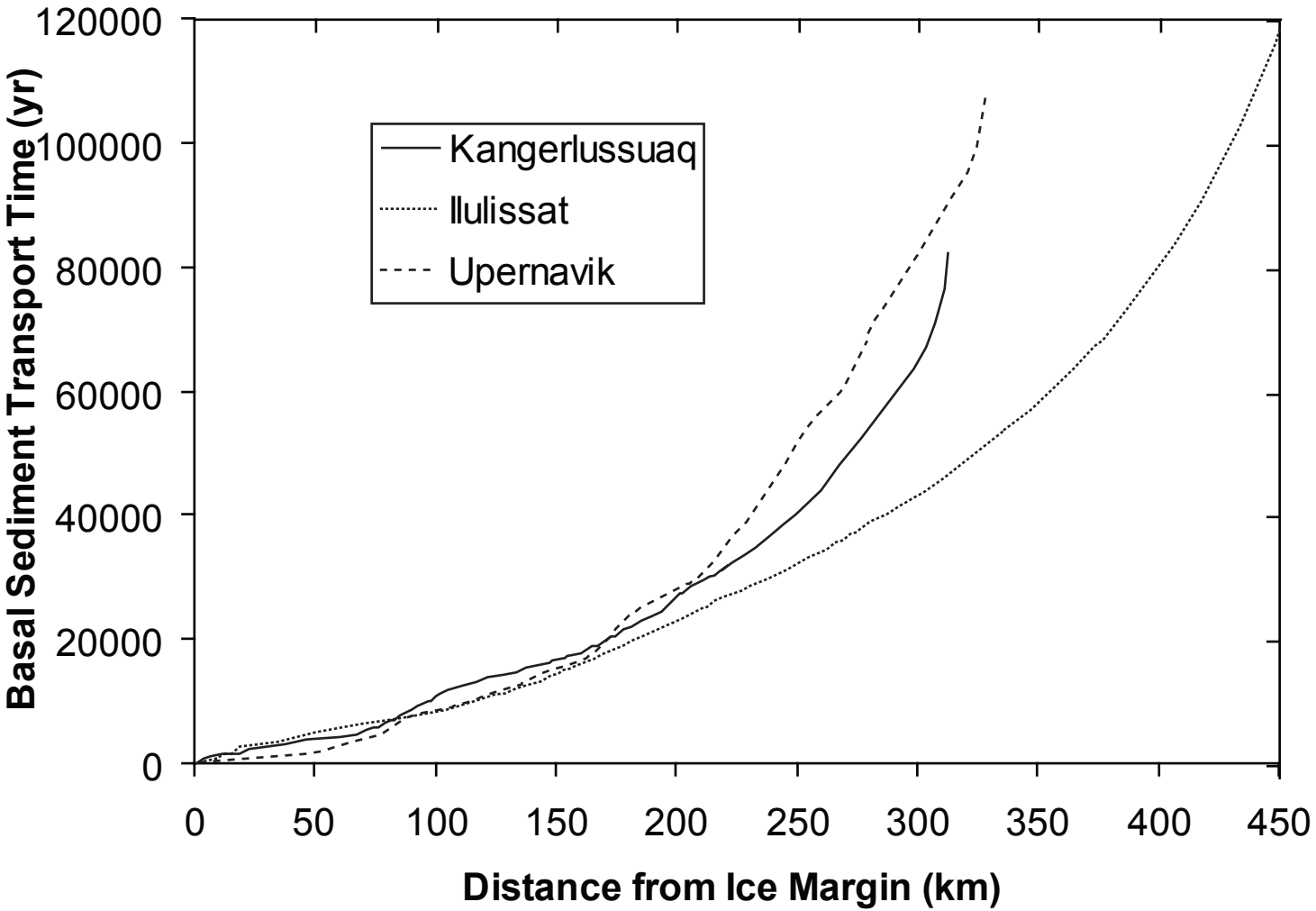
Basal Sediment Transport Time (yr)
120000
100000
80000
60000
40000
20000
0
0
50
100
150
200
250
300
350
400
450
Distance from Ice Margin (km)
Kangerlussuaq
Ilulissat
Upernavik

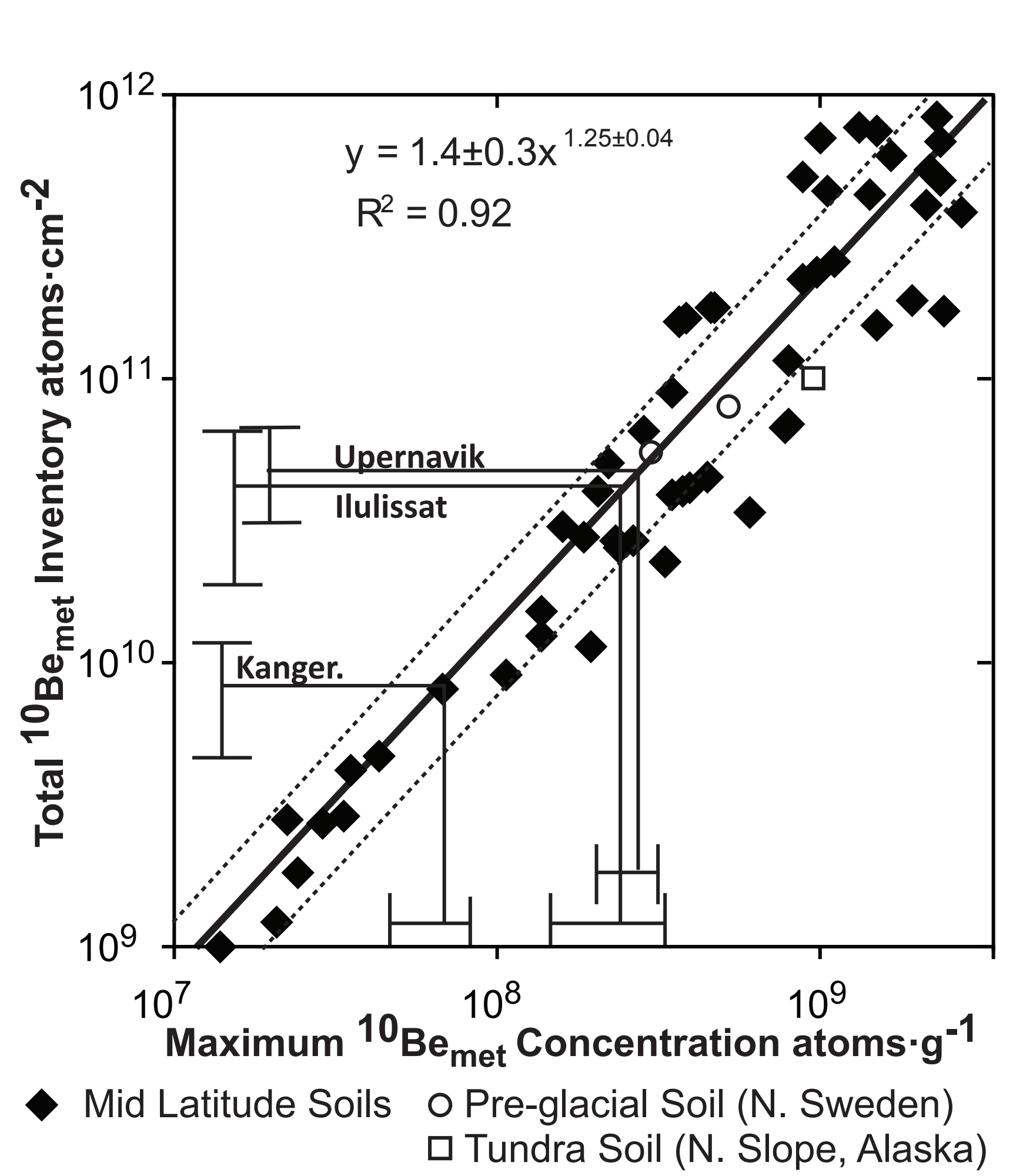
10^{12}
10^{11}
10^{10}
10^{9}
$y = 1.4\pm0.3x^{1.25\pm0.04}$
$R^2 = 0.92$
Upernavik
Ilulissat
Kanger.
Total $^{10}Be_{met}$ Inventory atoms·cm^{-2}
10^{7}
10^{8}
10^{9}
Maximum $^{10}Be_{met}$ Concentration atoms·g^{-1}
Mid Latitude Soils
Pre-glacial Soil (N. Sweden)
Tundra Soil (N. Slope, Alaska)